Supporting Information

for

Design, synthesis, and redox properties of donor-π-donor ferrocenyl functionalized phenothiazine derivatives

Deeksha Gupta[†],[a,b], Nikhil Ji Tiwari[†],[a], Prabal Pratap Singh[b], Rajneesh Misra[*,a]*

† Equally contributed as first authors.

* Corresponding Author

D. Gupta, N. J. Tiwari, R. Misra

[a]Department of Chemistry, Indian Institute of Technology Indore, Indore- 453552, India.

E-mail: rajneeshmisra@iiti.ac.in

P. P. Singh

[b]Department of Chemistry, GLA University17 km Stone, NH-2 Delhi-Mathura Highway, Chaumuhan, Mathura, Uttar Pradesh, India

Experimental Details

Chemicals were used as received unless otherwise indicated. All the oxygen- or moisture-sensitive reactions were carried out under an argon atmosphere, and the reflux reactions were performed in an oil bath. ^{1}H NMR (500 MHz) spectra were recorded on a Bruker 500 MHz FT-NMR spectrometer at room temperature. Chemical shifts are reported in delta (δ) units, expressed in parts per million (ppm) downfield from tetramethyl silane (TMS) using the deuterated solvents as an internal standard {$CDCl_3$, 7.26 ppm; DMSO-d_6, 2.50 ppm}. The Multiplicities are given as s (singlet), d (doublet), t (triplet) and m (multiplet) and the coupling constants, J, are given in hertz. ^{13}C NMR (126 MHz) on a Bruker 500 MHz FT-NMR spectrometer at room temperature. Chemical shifts are reported in delta (δ) un its, expressed in parts per million (ppm) downfield from TMS using the solvent as internal standard {$CDCl_3$, 77.16 ppm; DMSO-d_6, 39.52 ppm}. Thermogravimetric analysis was performed on the Mettler Toledo thermal analysis system. UV-visible absorption spectra of all compounds were recorded on a PerkinElmer Lambda 35 instrument in the DCM solution. All the measurements were carried out at 25 °C. HRMS were recorded on a Bruker-Daltonics micrOTOF-Q II mass spectrometer. The cyclic and differential pulse voltammograms (CVs and DPVs) were recorded on a PalmSens 4 electrochemical analyzer in the DCM solvent using glassy carbon as a working electrode, Pt wire as the counter electrode, and Ag/AgCl as the reference electrode. The scan rate was 100 mV s^{-1} for CV. A solution of tetrabutylammonium hexafluorophosphate ($[N(C_4H_9)_4]^+$ $[PF_6]^-$) in DCM (0.1 M) was used as the supporting electrolyte. Spectroelectrochemical measurements were done using a commercially available platinum honeycomb working electrode on a ceramic support in a narrow optical path quartz cuvette using a miniature Ag/AgCl gel electrode as a reference electrode. The potential was controlled and switched with a potentiostate. The resulting spectroscopic changes were measured with ALS SEC2020 spectrometer system. DFT calculations were performed using the B3LYP/6-31G(d,p) (B3LYP functional with the 6-31G(d,p) basis set) for C, H, S, O, and N atoms, and the LanL2DZ basis set for the Fe atom.[1]

Synthetic Scheme:

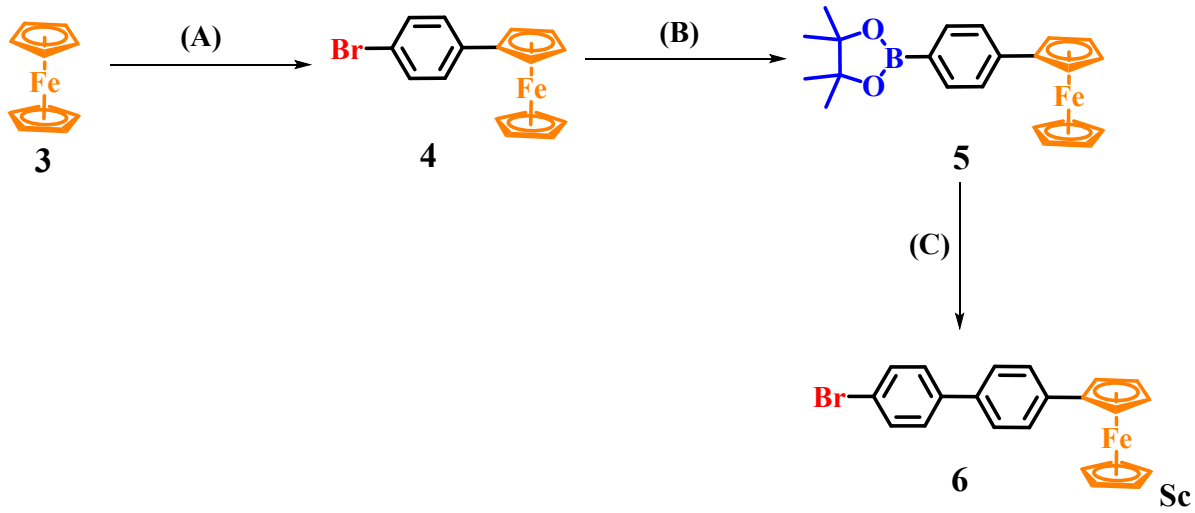

heme S1: (A) 4-bromo-aniline, $H_2SO_4/H_2O/NaNO_2$,

(B) Bis(pinacolato)diboron, KOAc, $[Pd(PPh_3)_4]$, toluene, reflux, 12 h

(C) 1-bromo-4-iodo-benzene, $[Pd(PPh_3)_4]$, THF:water, 60 °C, 16 h

Photophysical properties

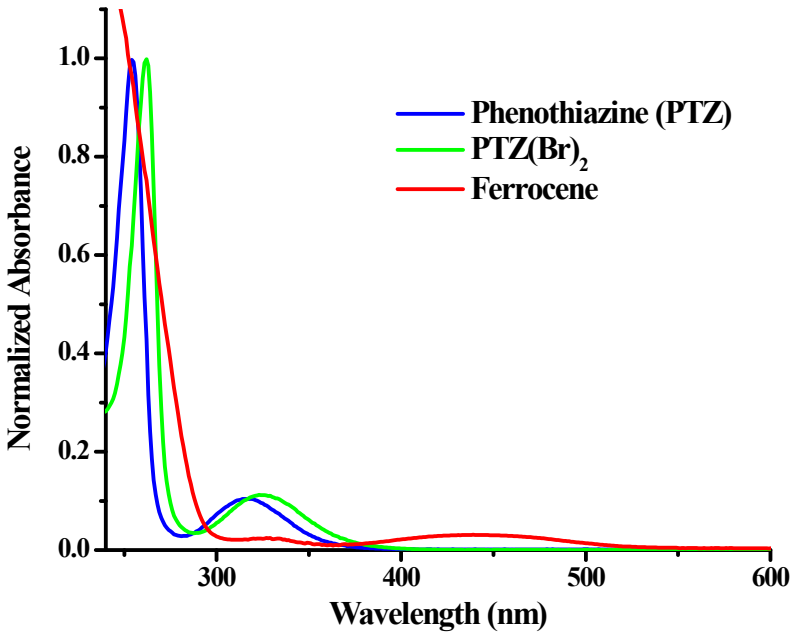

Fig. S1. Normalized electronic absorption spectra of **PTZ**, **PTZ(Br)$_2$**, and **Ferrocene** in Dichloromethane (1×10^{-5} M) at room temperature.

Density of State Analysis

In quantum mechanical analysis, the density of states (DOS) characterizes the distribution of energy levels per unit volume during electronic transitions. DOS plots illustrate cumulative energy states as the area beneath peaks in the spectrum, with high-intensity DOS indicates greater number of potential occupancy states at specific energy levels. The DOS analysis revealed that the electron delocalization occurs in the HOMO and LUMO orbitals due to the presence of molecular units. DOS calculations for the ferrocenyl functionalized phenothiazine derivatives **Fc1–4** was performed using the B3LYP/6-31G(d,p) level, with the results shown in Fig. S2. A zero DOS indicates the system cannot occupy any states. To better understand the DOS calculations of donor-π-donor derivatives **Fc1–4**, each ferrocenyl functionalized phenothiazine derivative was divided into three segments: PTZ (red), Fc (blue), and π-spacer (pink). All the phenyl spacers and ferrocenyl units of compounds **Fc1–4** are treated as a single fragment, indicated by Fc and π-spacer, respectively.

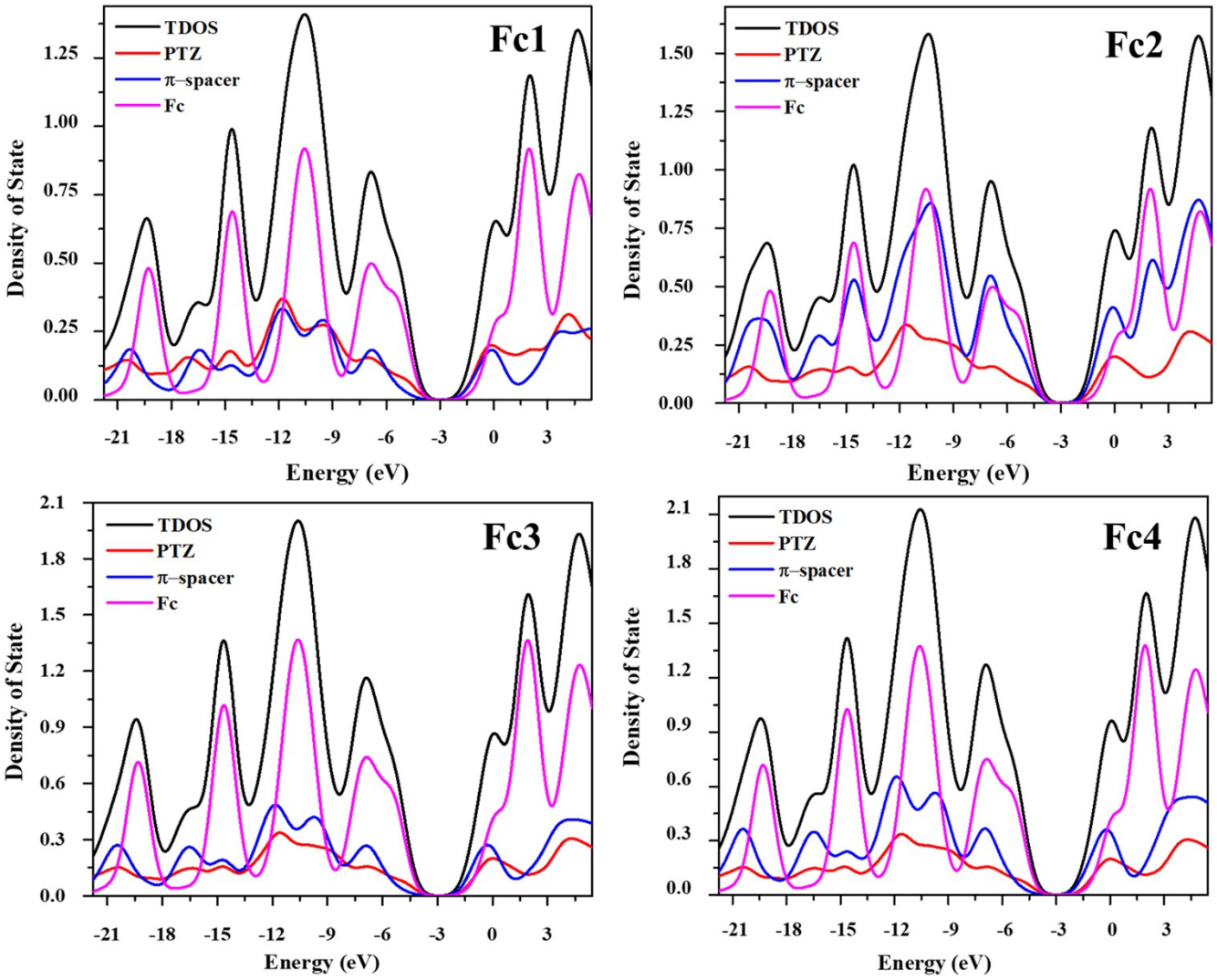

Fig. S2. Density of state (DOS) analysis of ferrocenyl functionalized phenothiazine derivatives **Fc1–4**.

The DOS plots display molecular orbital energy levels along the x-axis. Peaks with negative values on the left-side reflect the electronic cloud on the HOMOs, while peaks on the right-side with positive values represent the electronic cloud on the LUMOs. The distance between the left and right peaks indicates the energy difference between HOMO and LUMO. The y-axis depicts the relative strength of states. The DOS plots show significant contributions from the phenothiazine, phenyl spacer, and ferrocenyl units to the HOMO and LUMO levels. The observed energy gap in the DOS plot correlates well with the energy gap determined through density functional theory (DFT) calculations. Fluctuations in peak height within the DOS plot arise from electron mobility between the ferrocenyl and phenothiazine moieties, leading to changes in peak intensity at different energy levels.

FTIR spectroscopic analysis:

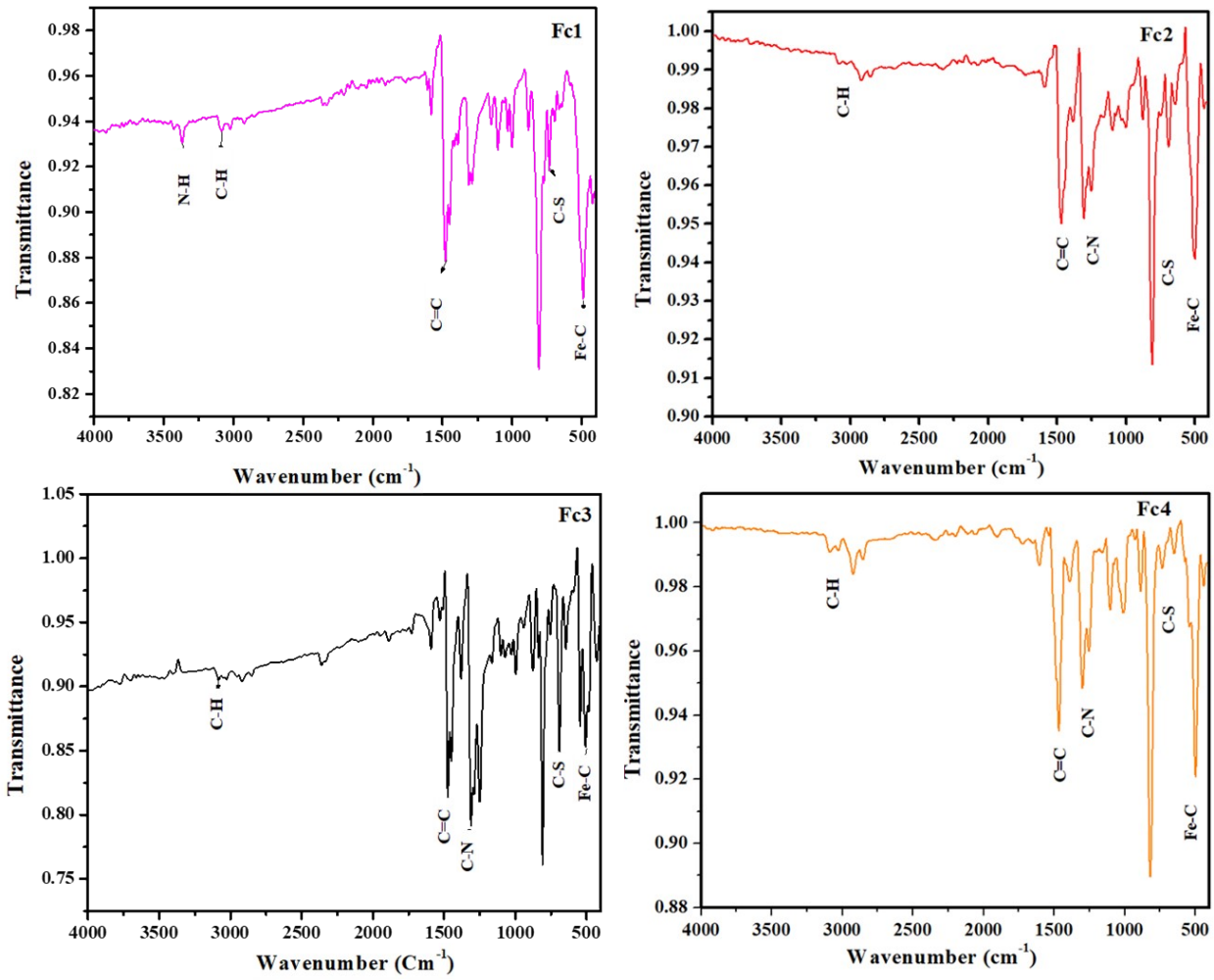

Fig. S3. FTIR spectra of ferrocenyl functionalized phenothiazine derivatives **Fc1–4**.

Differential Scanning Calorimetry:

For **Fc1**, an endothermic peak was observed at ~338 °C. This peak corresponds to the melting temperature of the **Fc1** derivative, indicating the transition from the crystalline solid phase to the molten phase. **Fc2** also exhibited an endothermic peak at ~321 °C. The observed peak at 321 °C confirms the transition from the crystalline phase to the molten state for **Fc2**. The higher melting temperature reflects the enhanced thermal stability of **Fc1**.

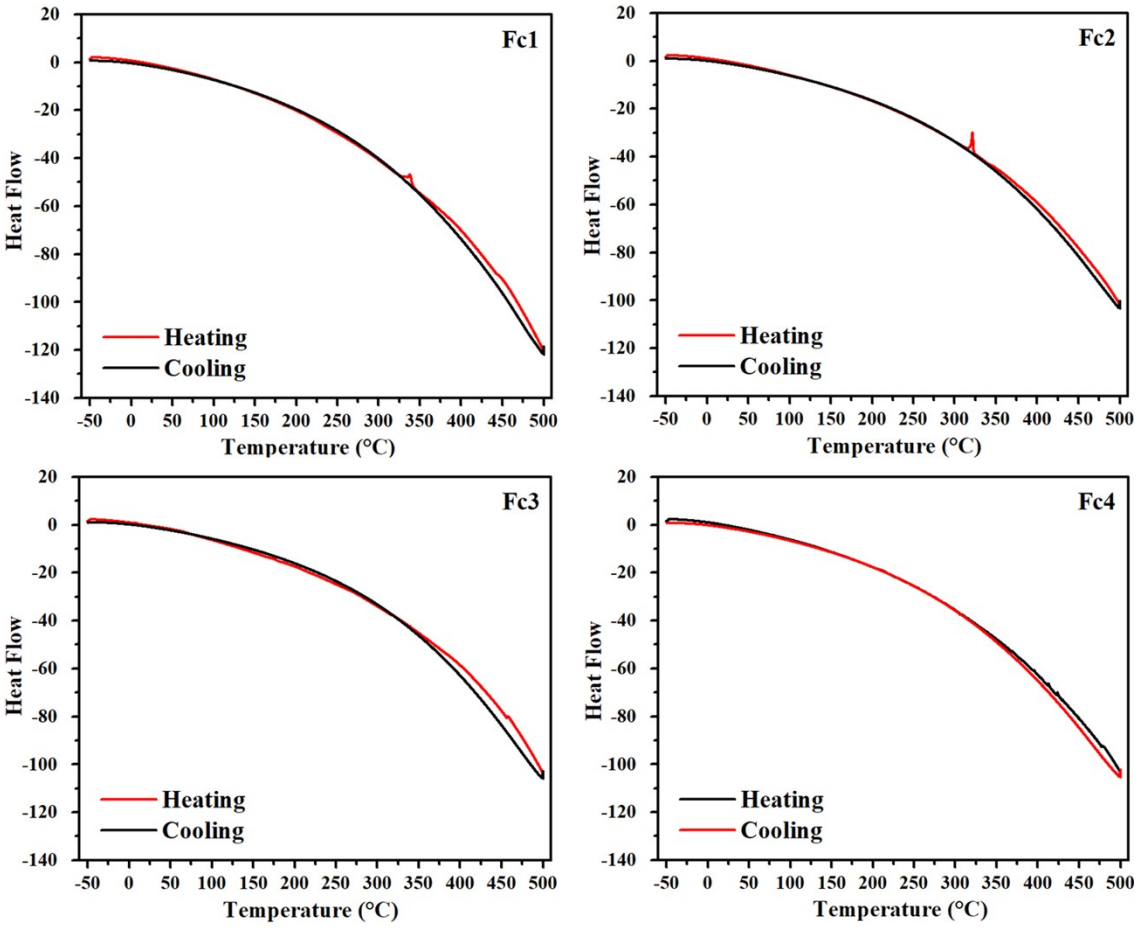

Fig. S4. Differential scanning colorimetry analysis of **Fc1–4** measured at a heating rate of 10 °C min^{-1} under nitrogen atmosphere.

Differential Pulse Voltammetry:

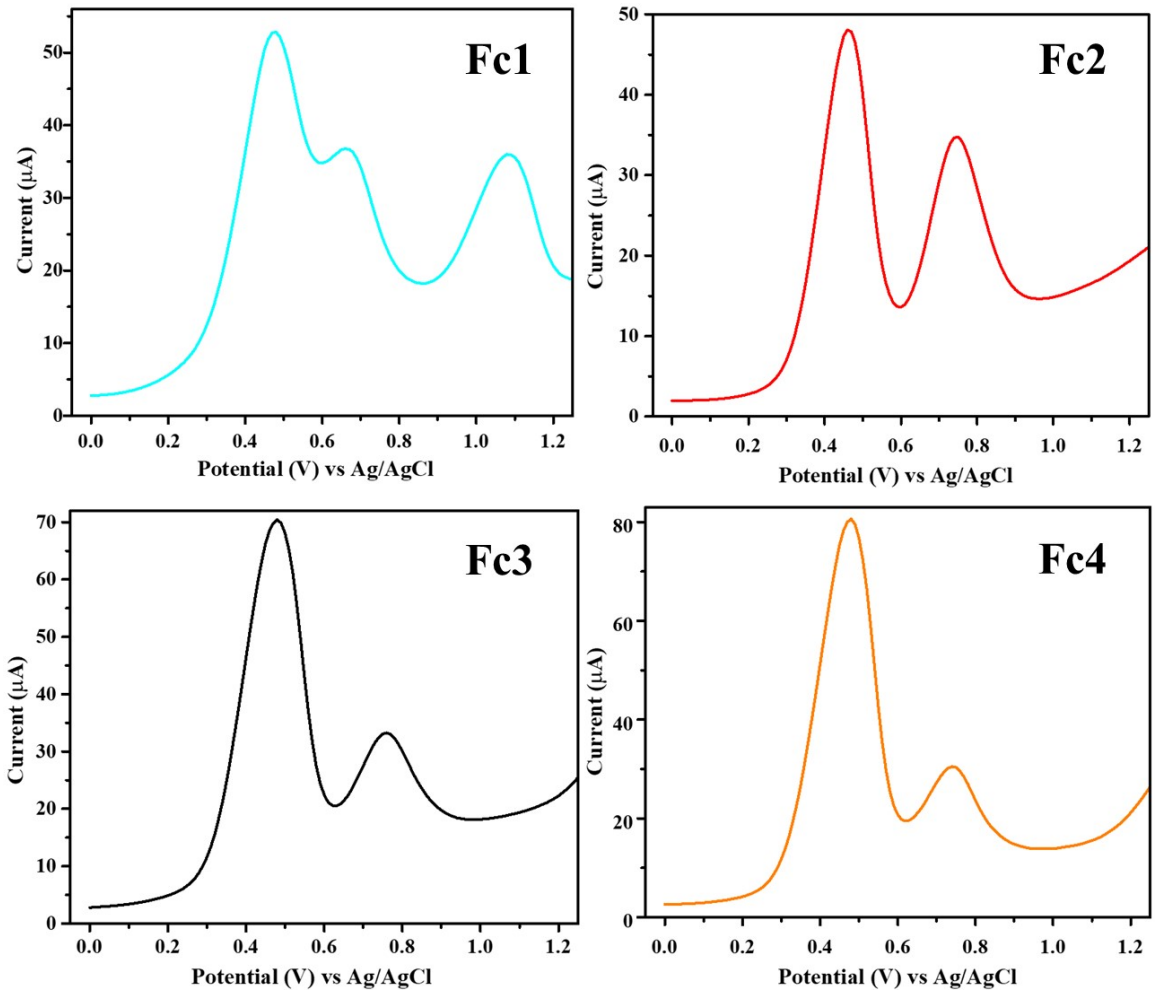

Fig. S5. Differential pulse voltammograms of **Fc1–4** in 0.1 M solution of $[N(C_4H_9)_4]^+$ $[PF_6]^-$ in dichloromethane at 100 mV s^{-1} scan rate versus Ag/AgCl at 25 °C.

Energy levels diagram of the frontier orbitals

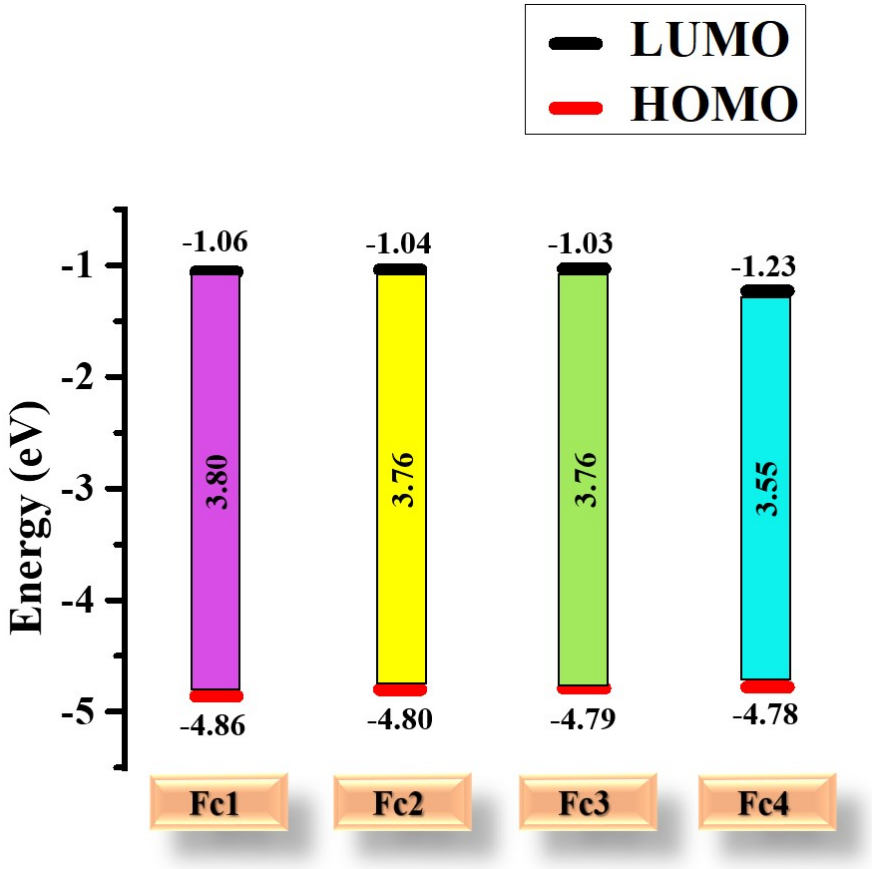

Fig. S6. Energy levels diagram of the frontier orbitals of **Fc1–4** estimated by DFT calculations.

(a)

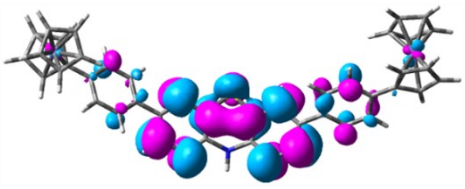

LUMO+3

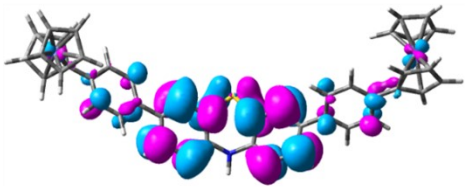

LUMO+2

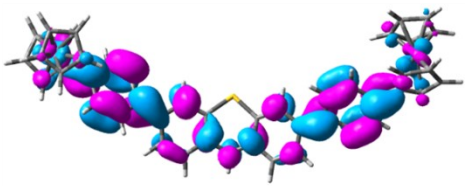

LUMO+1

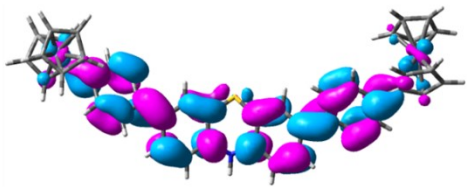

LUMO

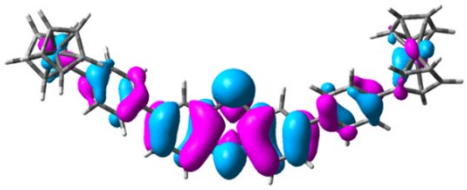

HOMO

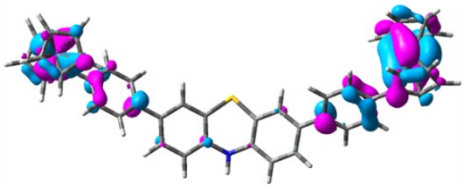

HOMO-1

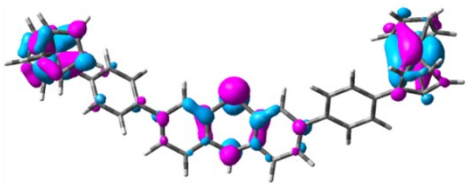

HOMO-2

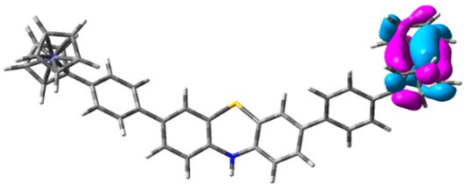

HOMO-3

(b)

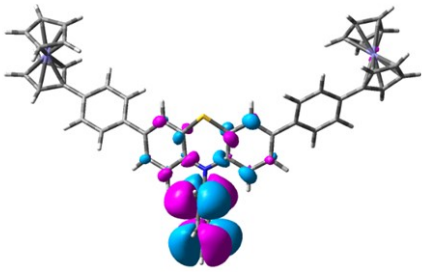

LUMO+3

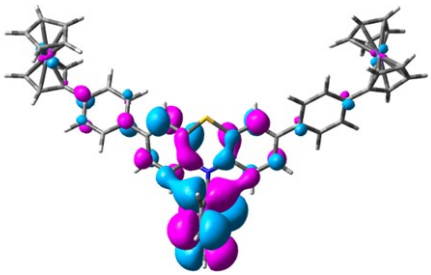

LUMO+2

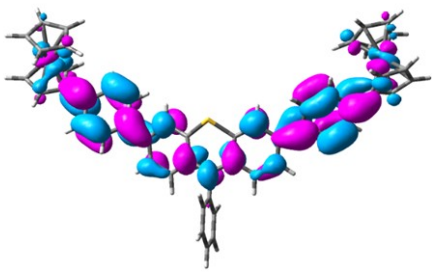

LUMO+1

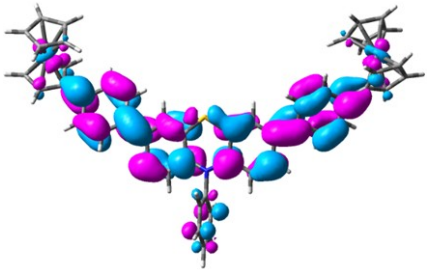

LUMO

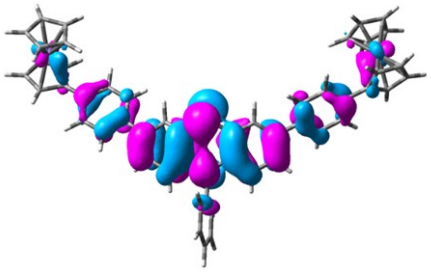

HOMO

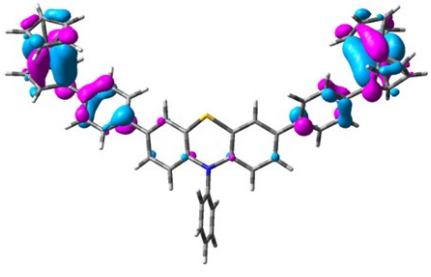

HOMO-1

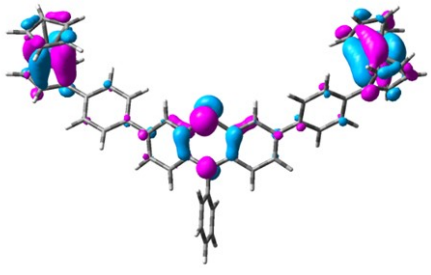

HOMO-2

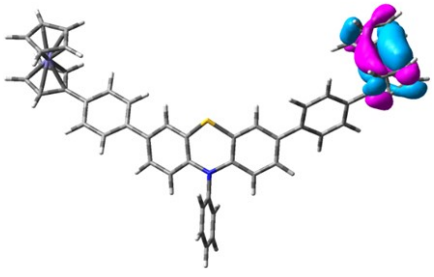

HOMO-3

(c)

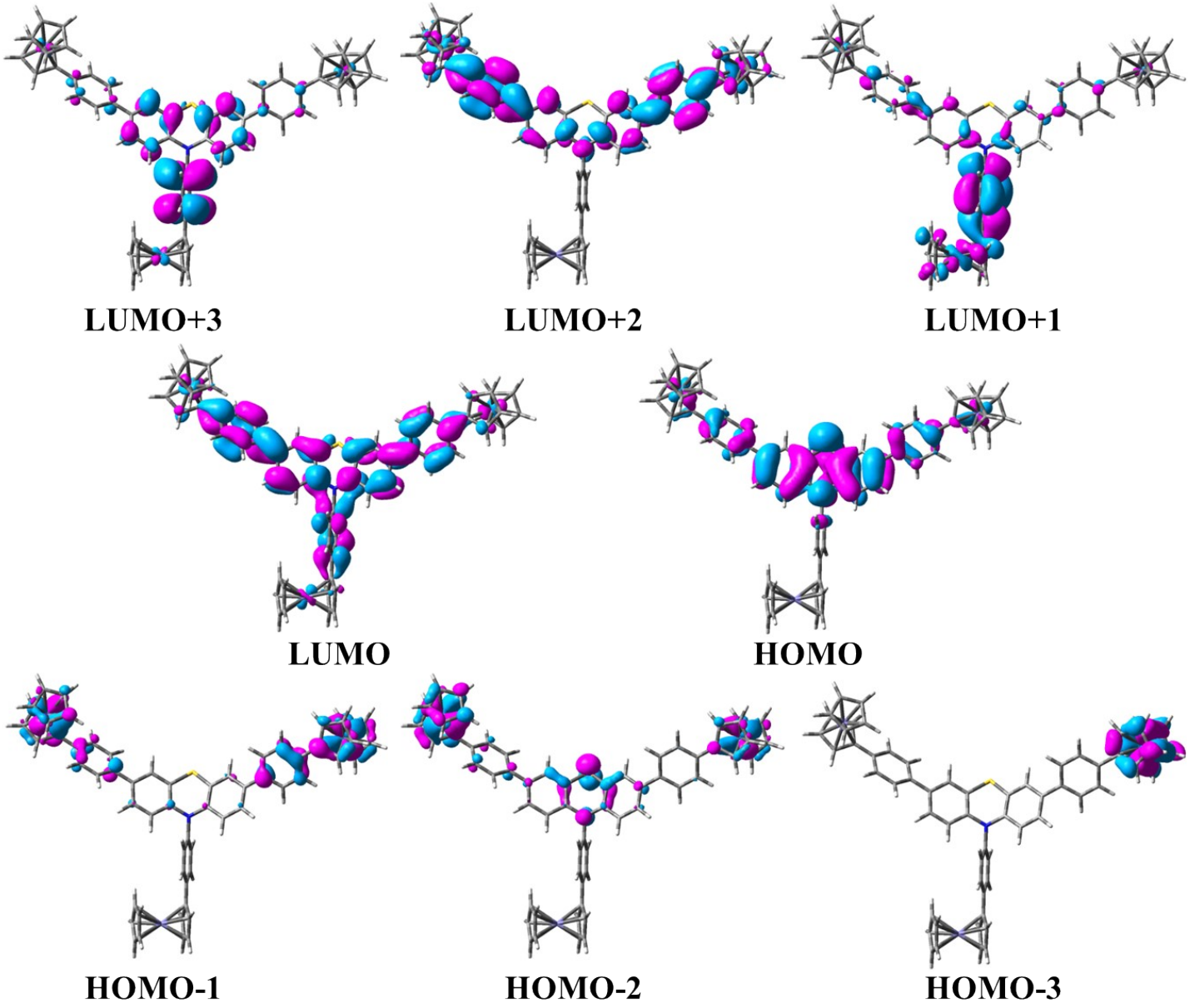

(d)

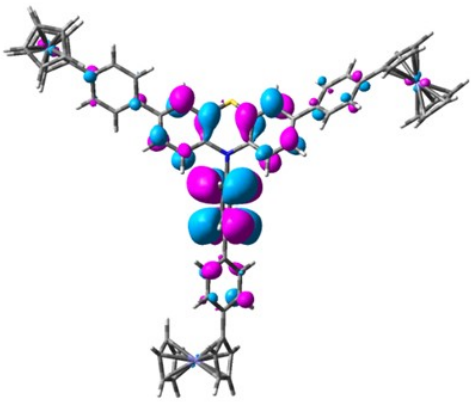

LUMO+3

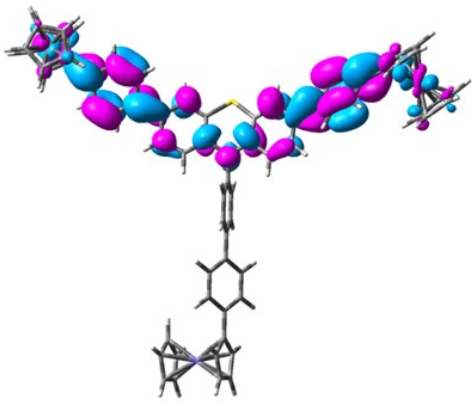

LUMO+2

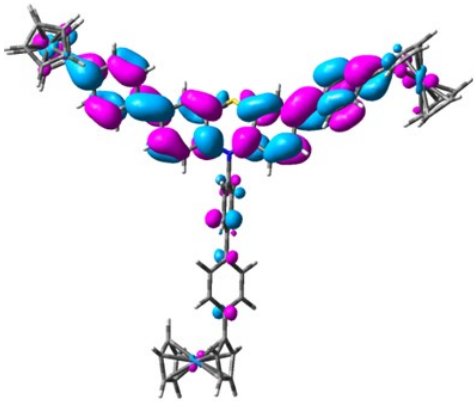

LUMO+1

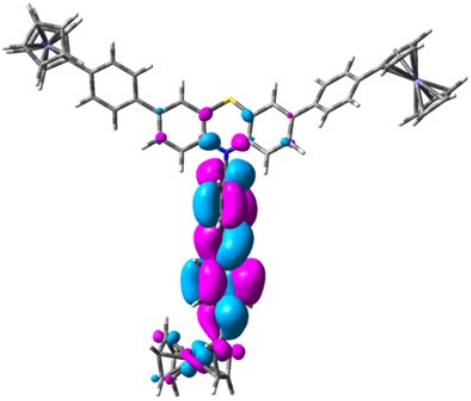

LUMO

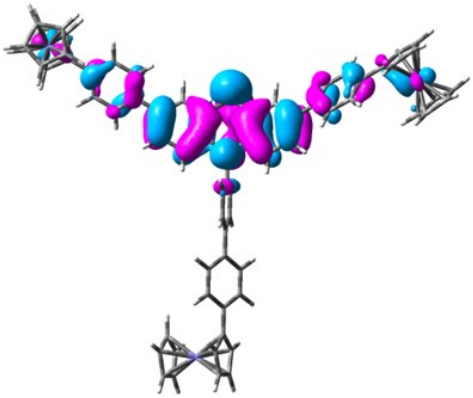

HOMO

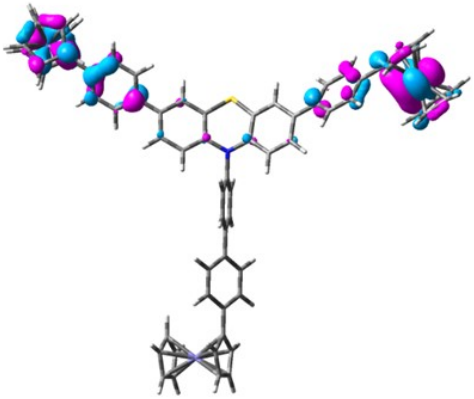

HOMO-1

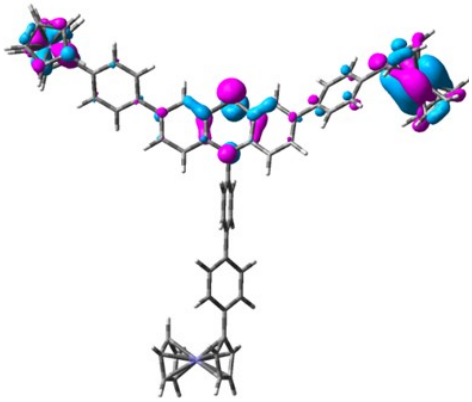

HOMO-2

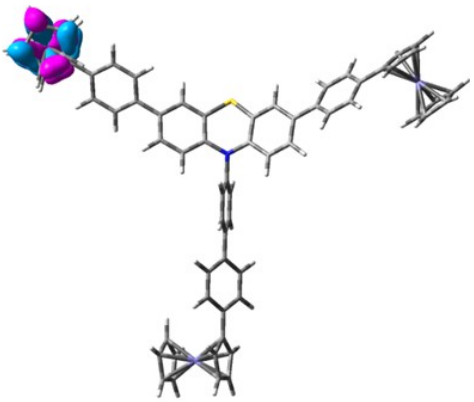

HOMO-3

Fig. S7. The molecular orbitals of (a) **Fc1**, (b) **Fc2**, (c) **Fc3**, and (d) **Fc4** are estimated from DFT calculation.

Single Crystal x-ray Diffraction Studies:

Single crystal x-ray structural studies of **Fc2** and **Fc3** were performed on a CCD Agilent Technologies (Oxford Diffraction) SUPER NOVA diffractometer. Data were collected at 293(2) K using graphite-monochromated Mo Kα radiation (λ_α = 0.71073 Å). Unit cell determination, data collection and reduction, and empirical absorption correction were performed using the CrysAlisPro program. The data were collected by the standard 'phi-omega scan techniques, and were scaled and reduced using CrysAlisPro RED software. The Olex 2–1.5 program[2] was used as the graphical interface. The structures were solved by direct methods using SHELXT,[3] which revealed the positions of all not disordered non-hydrogen atoms. The structure model was refined using full matrix least squares minimization on F^2 using ShelXL[4] within Olex2 for a graphical interface. The positions of all the atoms were obtained by direct methods. All non-hydrogen atoms were refined anisotropically. The remaining hydrogen atoms were placed in geometrically constrained positions, and refined with isotropic temperature factors, generally 1.2U_{eq} of their parent atoms. The crystal and refinement data are summarized in Table S1. The CCDC numbers **2376697** and **2376607** contain the supplementary crystallographic data for **Fc2** and **Fc3** respectively. These data can be obtained free of charge via www.ccdc.cam.ac.uk/conts/retrieving.html (or from the Cambridge Crystallographic Data Centre, 12 union Road, Cambridge CB21 EZ, UK; Fax: (+44) 1223-336 033; or deposit@ccdc.cam.ac.uk).

Single Crystal x-ray Analysis

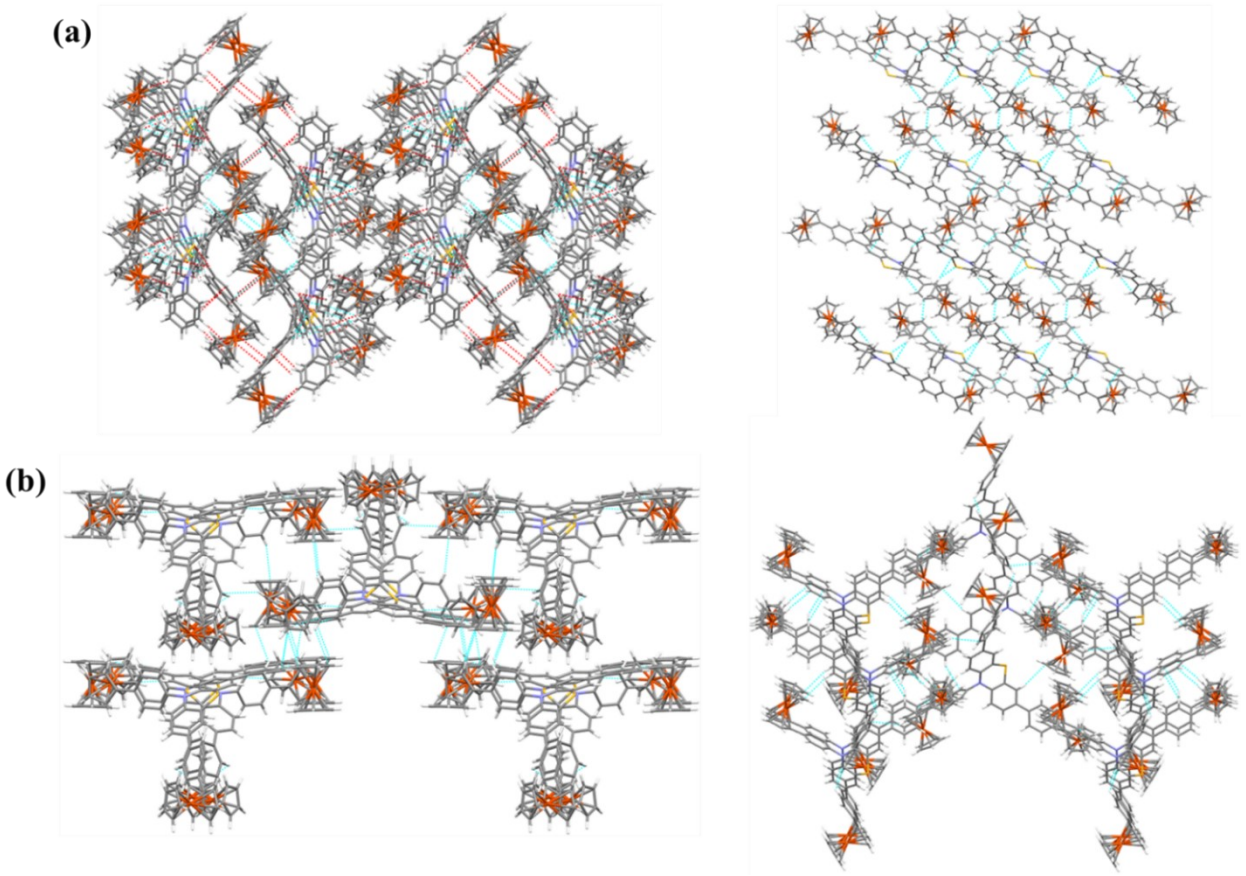

Fig. S8. Crystal packing diagrams of the (a) **Fc2** and (b) **Fc3**.

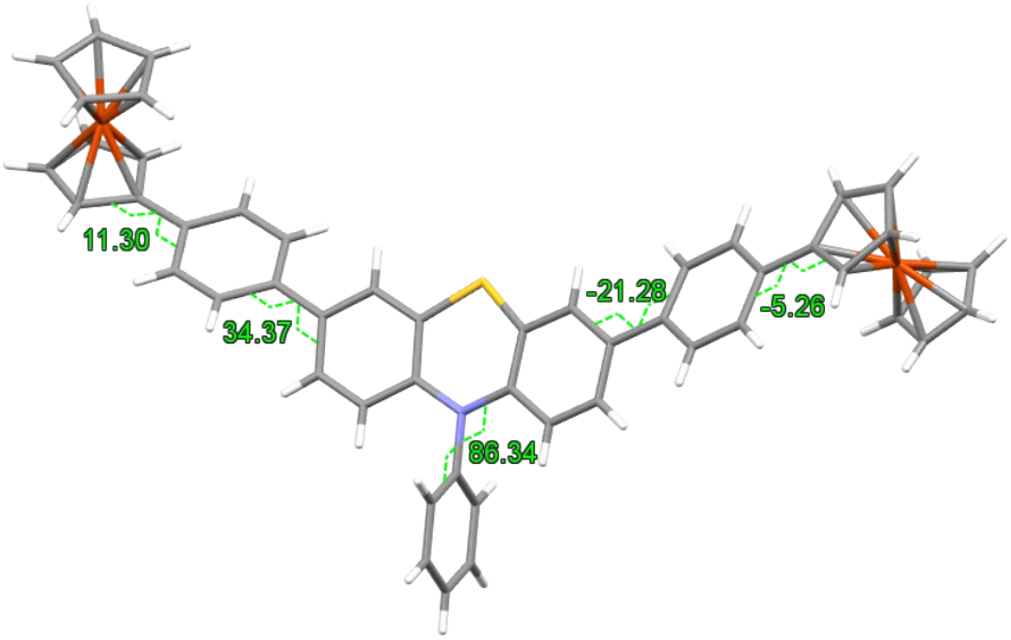

Fc2

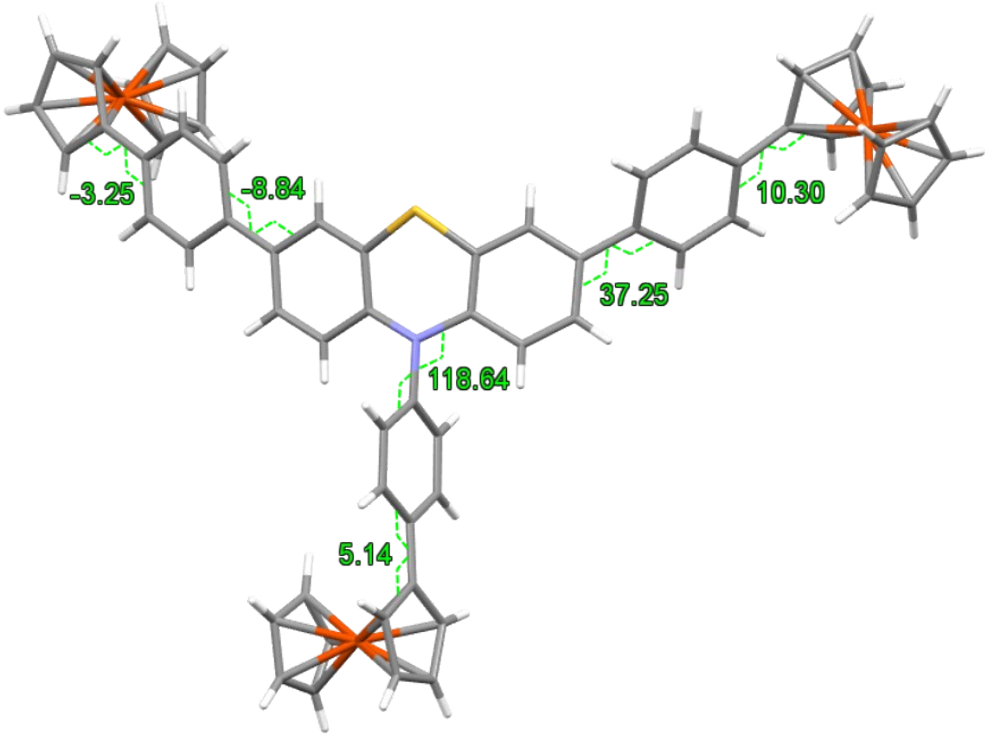

Fc3

Fig. S9. Torsion angles between the key atoms of phenothiazine, phenyl, and ferrocenyl unit of the **Fc2** and **Fc3**.

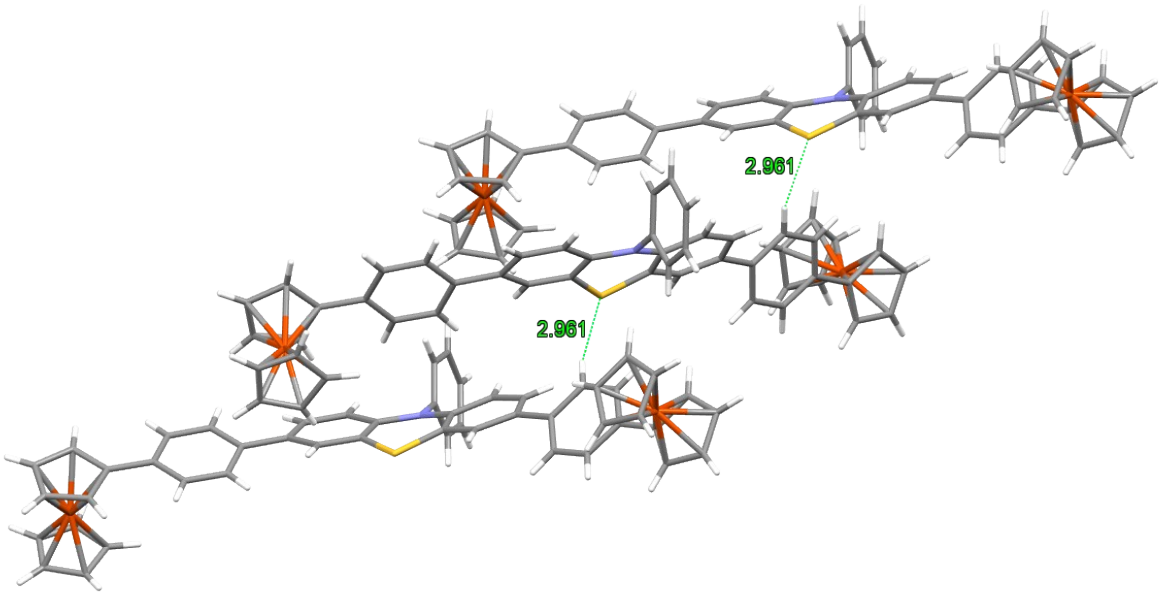

Fig. S10. S–H hydrogen bonding interactions between the packing diagram of **Fc2**.

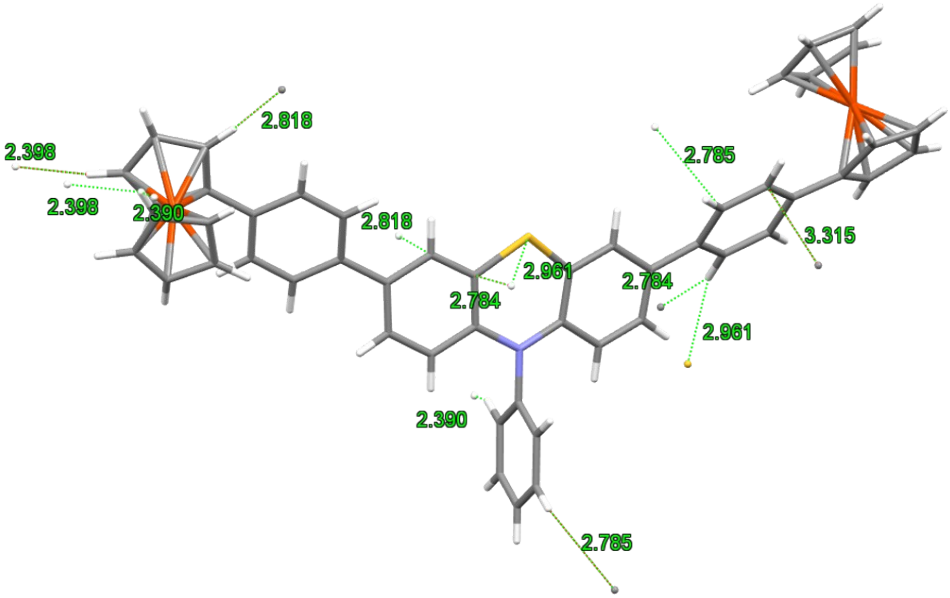

Fc2

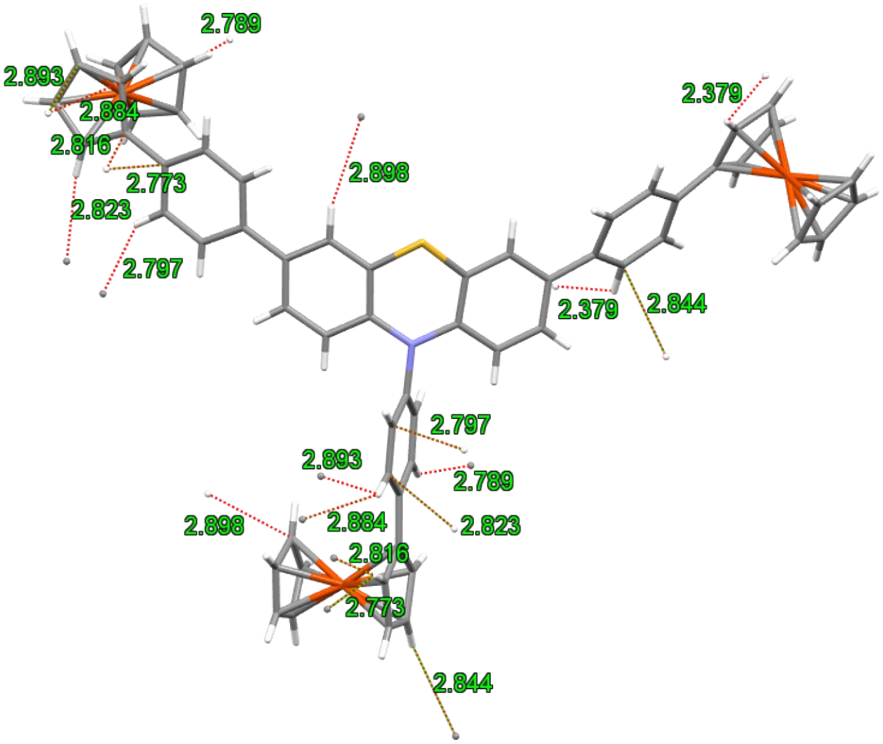

Fc3

Fig. S11. All the different intermolecular interactions between the molecules of **Fc2** and **Fc3**.

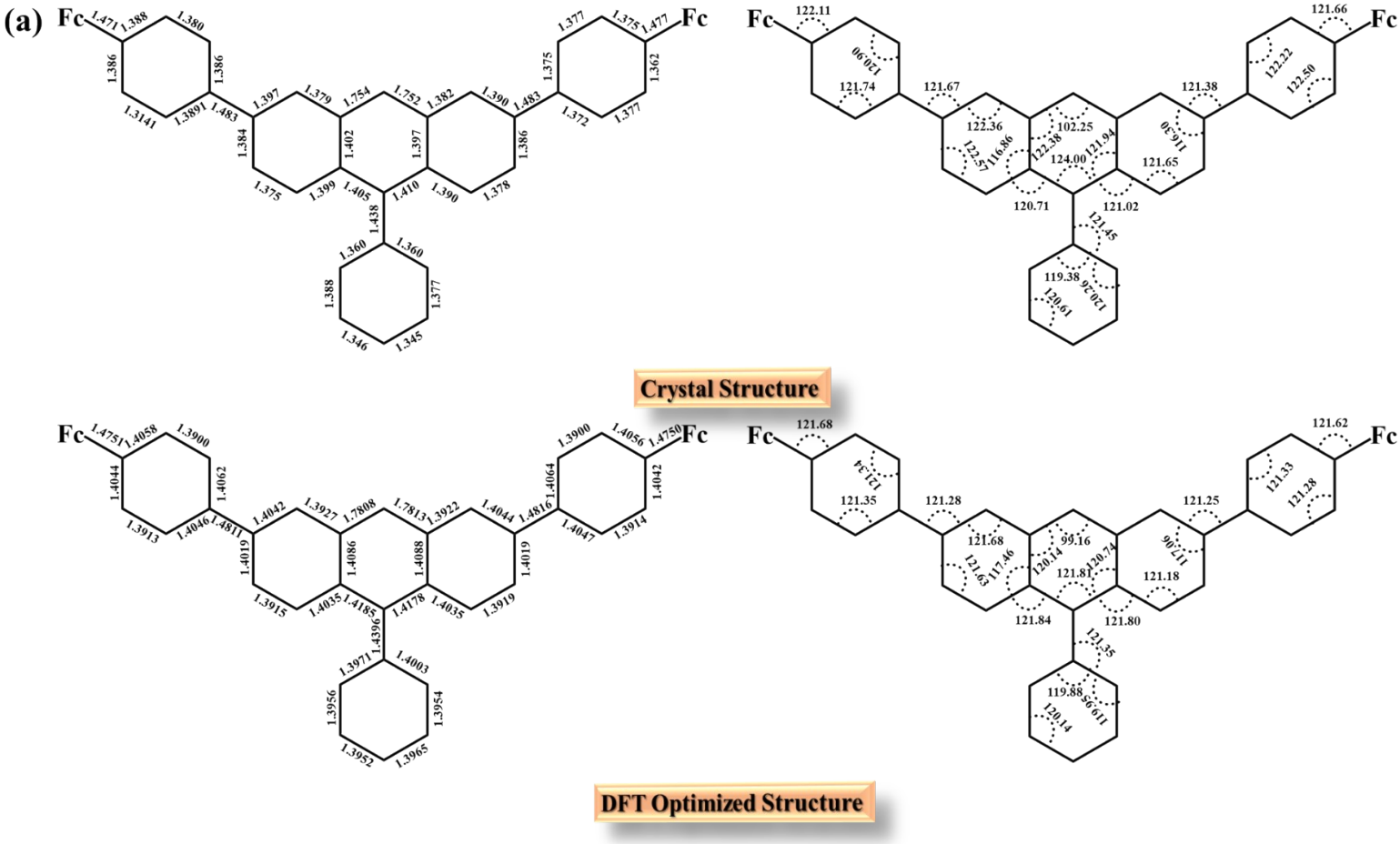
(a)
Fc
Fc
1.471
1.388
1.380
1.386
1.386
1.3141
1.3891
1.483
1.384
1.397
1.379
1.754
1.752
1.382
1.390
1.483
1.375
1.377
1.375
1.477
1.362
1.372
1.377
1.386
1.375
1.399
1.405
1.410
1.390
1.378
1.438
1.360
1.360
1.388
1.377
1.346
1.345
122.11
121.74
120.90
121.67
122.36
122.38
102.25
121.94
124.00
121.38
116.30
121.65
121.66
122.22
122.50
120.71
121.02
121.45
119.38
120.61
120.26
Crystal Structure
Fc
Fc
1.4751
1.4058
1.3900
1.4044
1.4062
1.3913
1.4046
1.4811
1.4019
1.4042
1.3927
1.7808
1.7813
1.3922
1.4044
1.4816
1.4064
1.3900
1.4056
1.4750
1.4042
1.4047
1.3914
1.4086
1.4088
1.4019
1.3915
1.4035
1.4185
1.4178
1.4035
1.3919
1.4396
1.3971
1.4003
1.3956
1.3954
1.3952
1.3965
121.68
121.35
121.24
121.28
121.68
121.63
117.46
120.14
99.16
120.74
121.81
121.25
121.62
121.33
121.28
117.06
121.18
121.84
121.80
121.35
119.88
120.14
119.96
DFT Optimized Structure

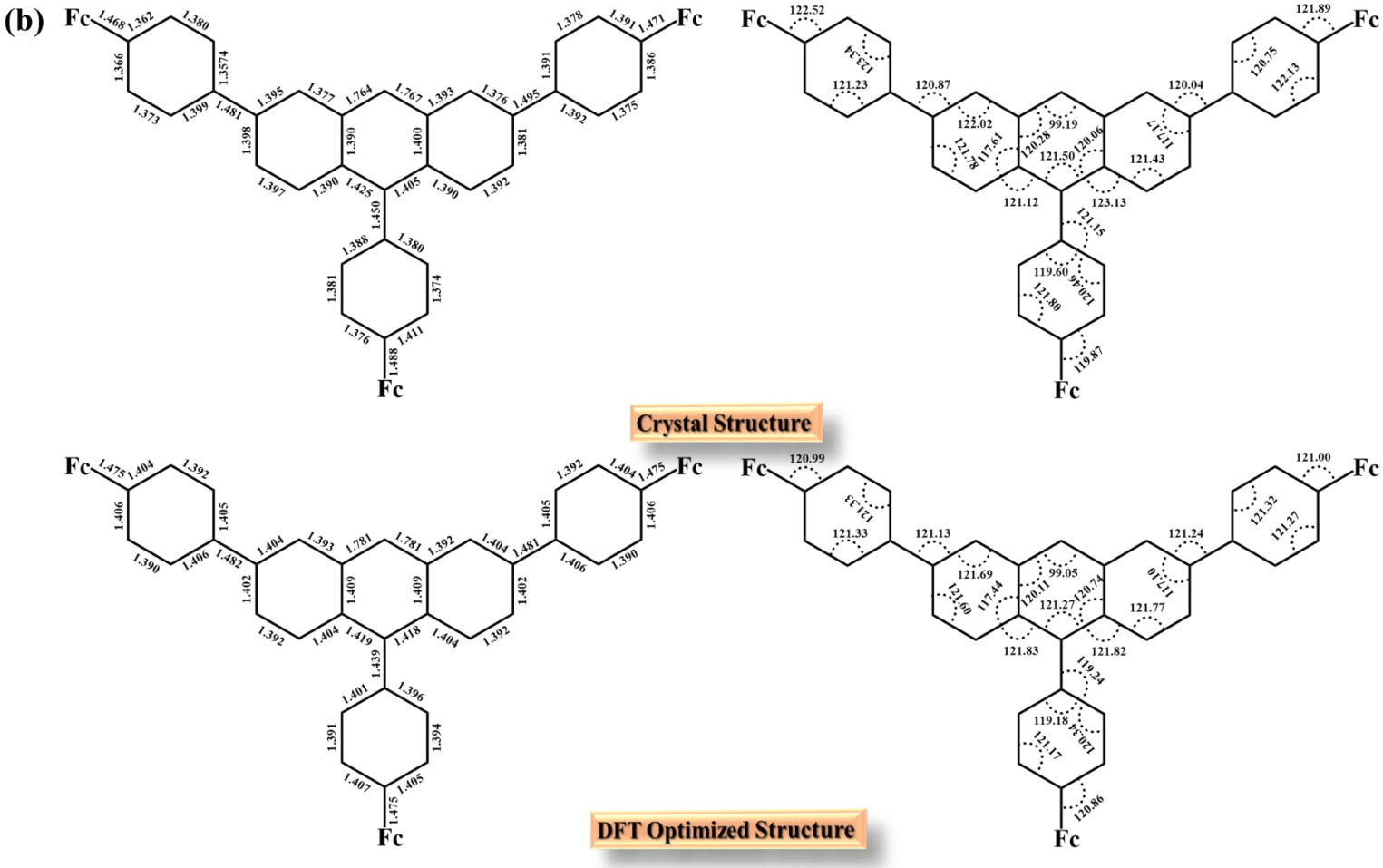
(b)
Fc
Fc
Fc
Fc
Crystal Structure
Fc
Fc
Fc
Fc
DFT Optimized Structure

Fig. S12. Comparable study of bond lengths and bond angles of the crystal structures and DFT optimized structures of the ferrocenyl functionalized phenothiazine derivatives (a) **Fc1** and (b) **Fc3**.

Table S1. Crystal data and structure refinement for PTZ 1–3.

	Fc2	**Fc3**
Identification Code	2376697CIF Revised	2376607CIF Revised
Empirical Formula	$C_{50}H_{37}Fe_2NS$	$C_{61}H_{47}Cl_2Fe_3NS$
Formula Weight	795.50	1064.50
Temperature/K	293.00	293.00
Crystal System	monoclinic	monoclinic
Space Group	$P2_1/n$	$P2_1/c$
a/(Å)	21.8411 (5)	12.6310 (2)
b/(Å)	10.6895 (3)	26.5578 (5)
c/(Å)	16.3082 (3)	14.6540 (2)
α /(deg)	90	90
β/(deg)	91.229 (2)	91.099 (2)
γ/(deg)	90	90
Volume/ (Å)³	3806.61 (15)	4914.80 (14)
Z	4	4
Dx (Mg m⁻³)	1.388	1.439

F(000)	0.854	1.067
μ (mm^{-1})	1648.0	2092.0
Θ range for data collection(deg)	0.3 x 0.2 x 0.2	0.12 x 0.08 x 0.078
Limiting indices	Mo K*α* *(λ = 0.71073)*	Mo K*α* *(λ = 0.71073)*
Reflections collected	3.73 to 49.994	3.572 to 50
unique reflections	$-25 \leq h \leq 25$, $-12 \leq k \leq 12$, $-19 \leq 1 \leq 19$	$-15 \leq h \leq 15$, $-31 \leq k \leq 31$, $-17 \leq 1 \leq 17$
R(int)	58498	76112
Completeness to θ	6696 [R_{int} = 0.0411, R_{sigma} = 0.0275]	8612 [R_{int} = 0.0386, R_{sigma} = 0.0256]
Data/restraints/parameters	6696/0/495	8612/0/613
GOF on F^2	1.151	1.141
R1 and R2 [I>2σ(I)]	R_1=0.0395, wR_2 = 0.0989	R_1=0.0421, wR_2 = 0.1146
R1 and R2 (all data)	R_1 = 0.0564, wR_2 = 0.1048	R1=0.0555, wR2 = 0.1206
Largest diff. peak and hole(e.A^{-3})	0.52/-0.46	0.39/-0.58

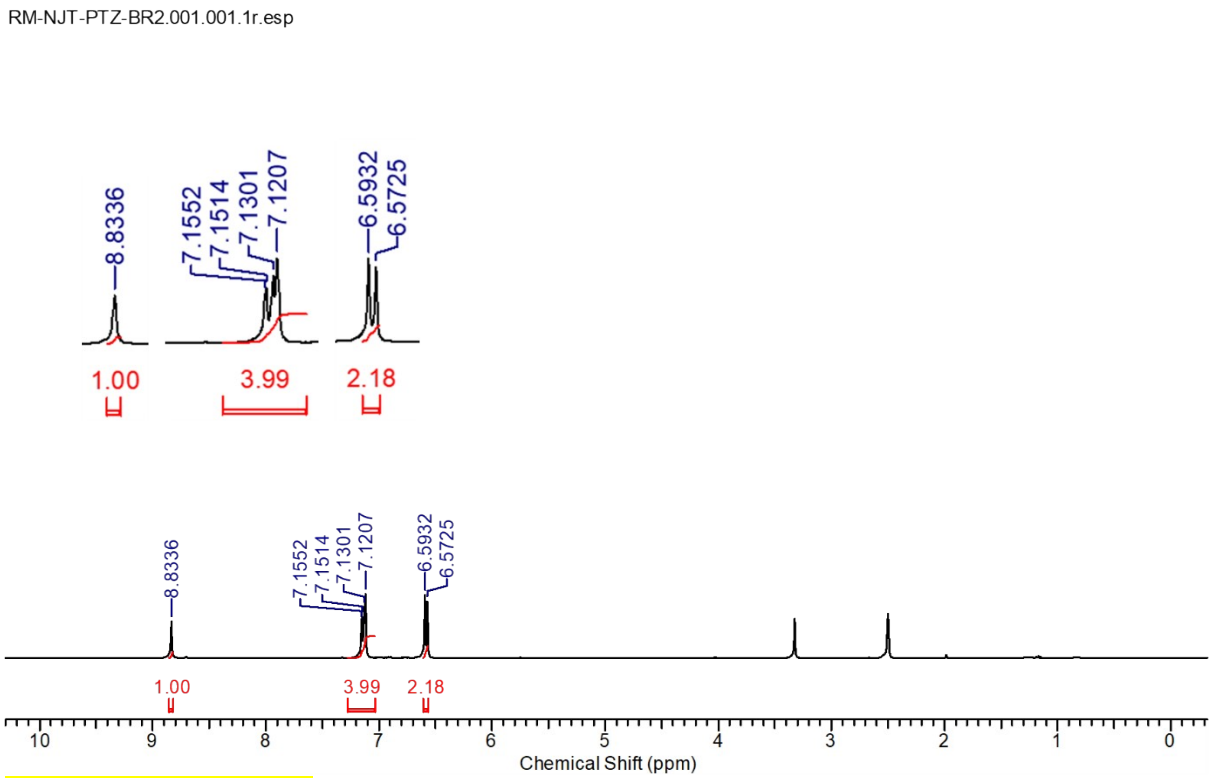

Fig. S13. ^{1}H NMR of **2**.

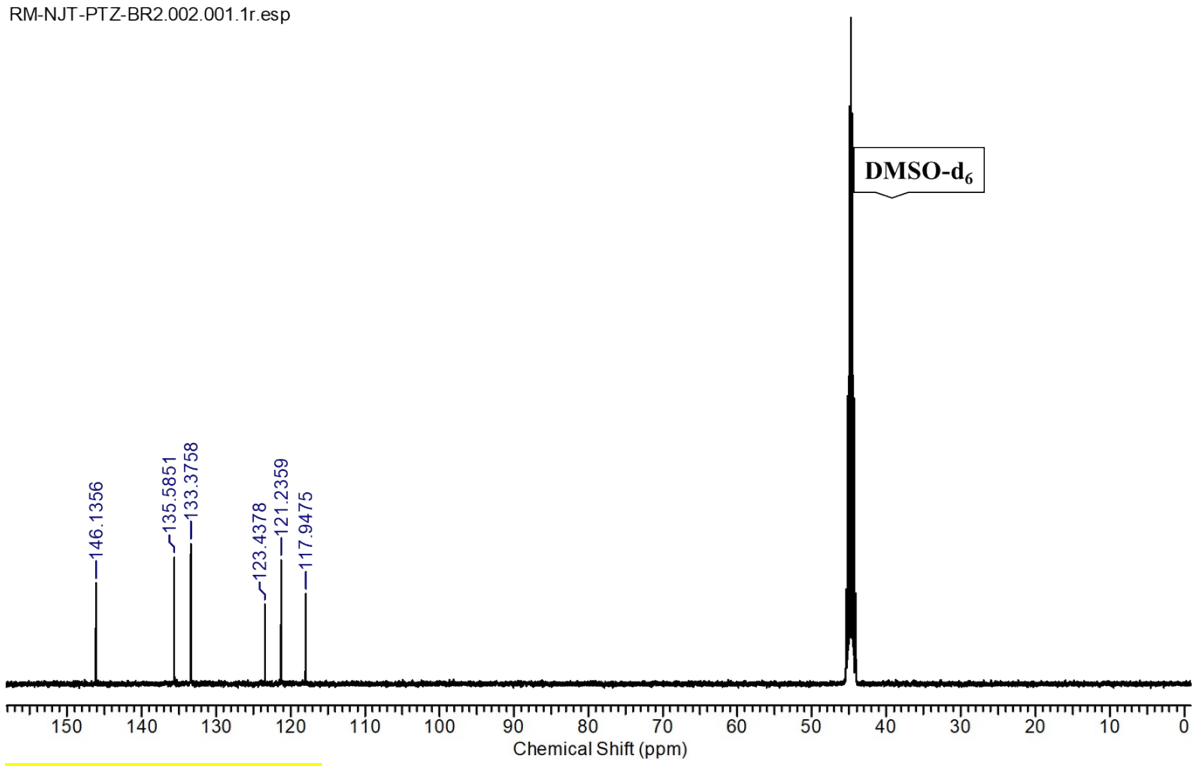

Fig. S14. ^{13}C NMR of **2**.

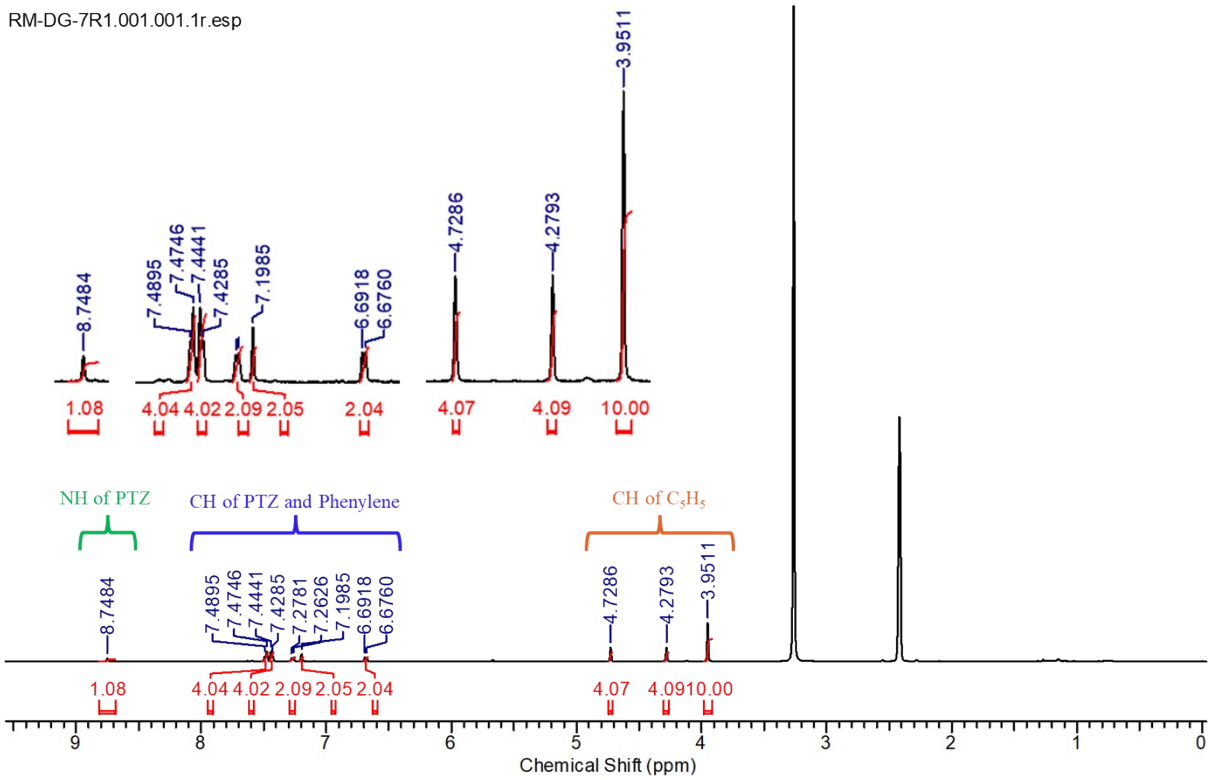

Fig. S15. ^{1}H NMR of **Fc1**.

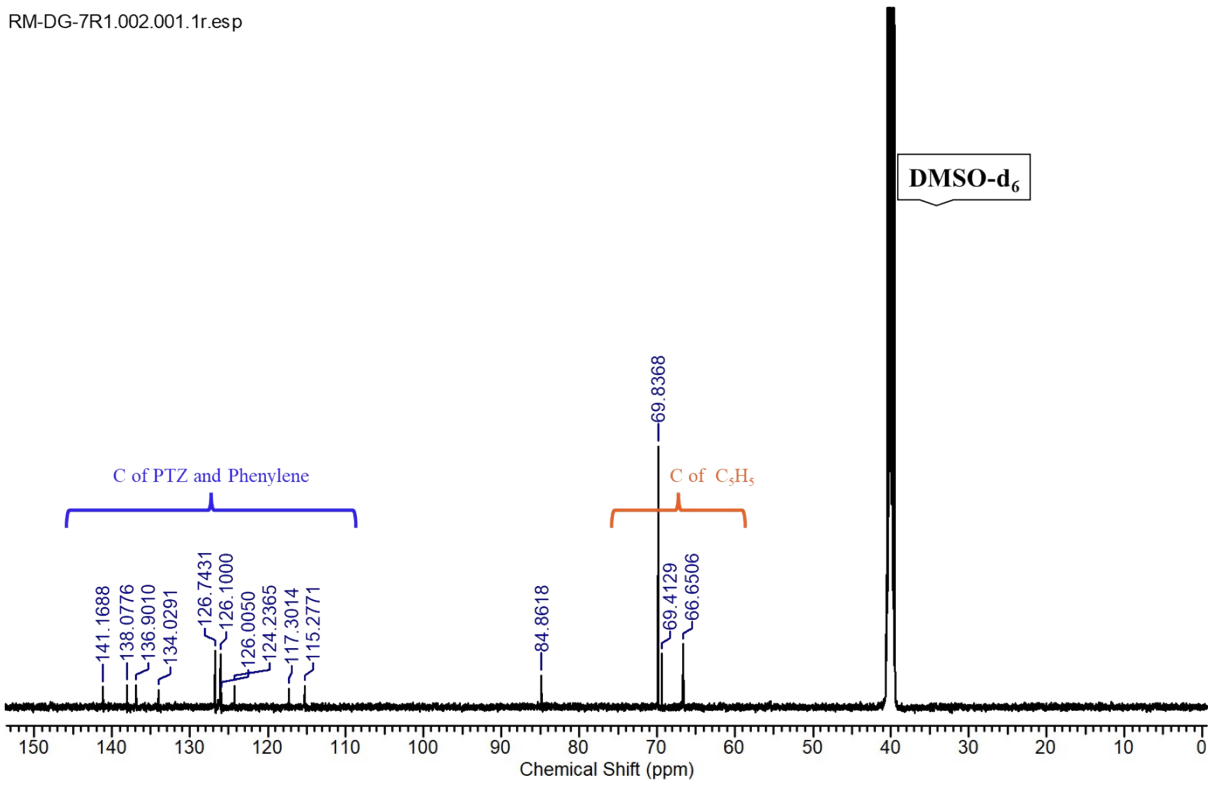

Fig. S16. ^{13}C NMR of **Fc1**.

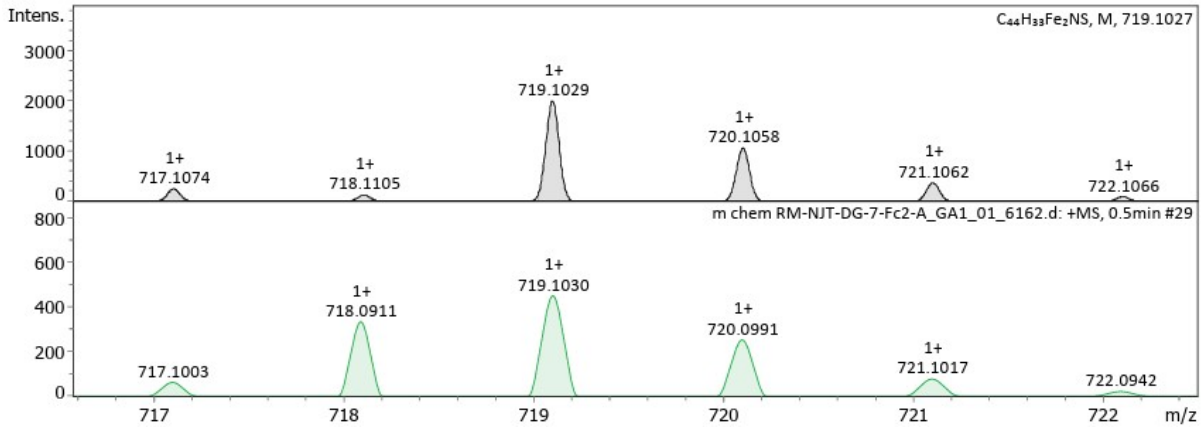

Fig. S17. HRMS of **Fc1**.

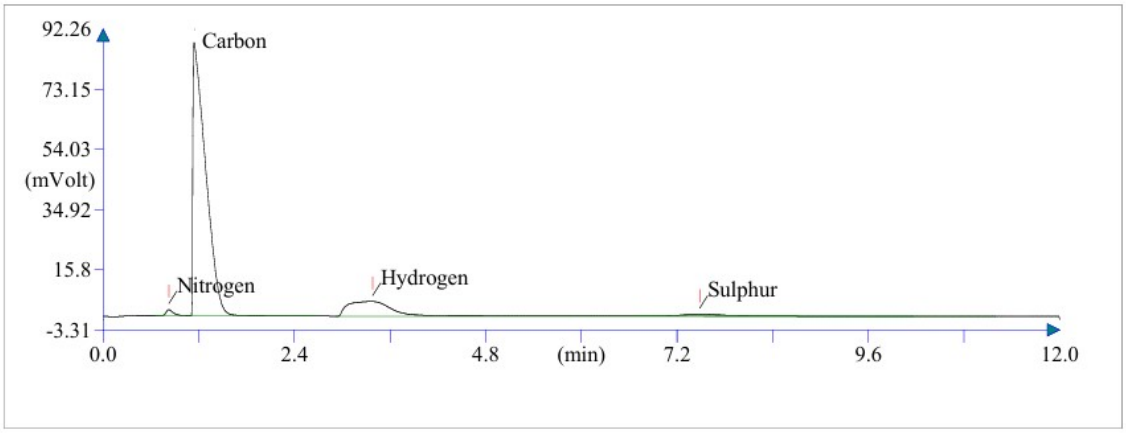

Operator ID:
Company name: ThermoFinnigan
Method filename: C:\Eager for FLASH\04 JUL 24 CHNS\NCHS_19-12-2024.mth
Method name: NCHS
Analysed: 22-01-25 12:23
Printed: 01-22-2025 15:05
Elemental Analyser method:
Sampler method:
Sample ID: RM-DG-Fc-1 (# 31)
Analysis type: UnkNown
Chromatogram filename: 22-01-25-02.dat
Calibration method: K Factors
Sample weight: 2.426
Protein factor: 6.25

Component Name	Element %	Retention Time (min)	Area (.1*uV*sec)
Nitrogen	1.886	0.825	130345
Carbon	71.845	1.142	9628271
Hydrogen	4.587	3.383	1849066
Sulphur	4.390	7.483	233958
	82.708		11841640

Fig. S18. Elemental analysis of **Fc1**.

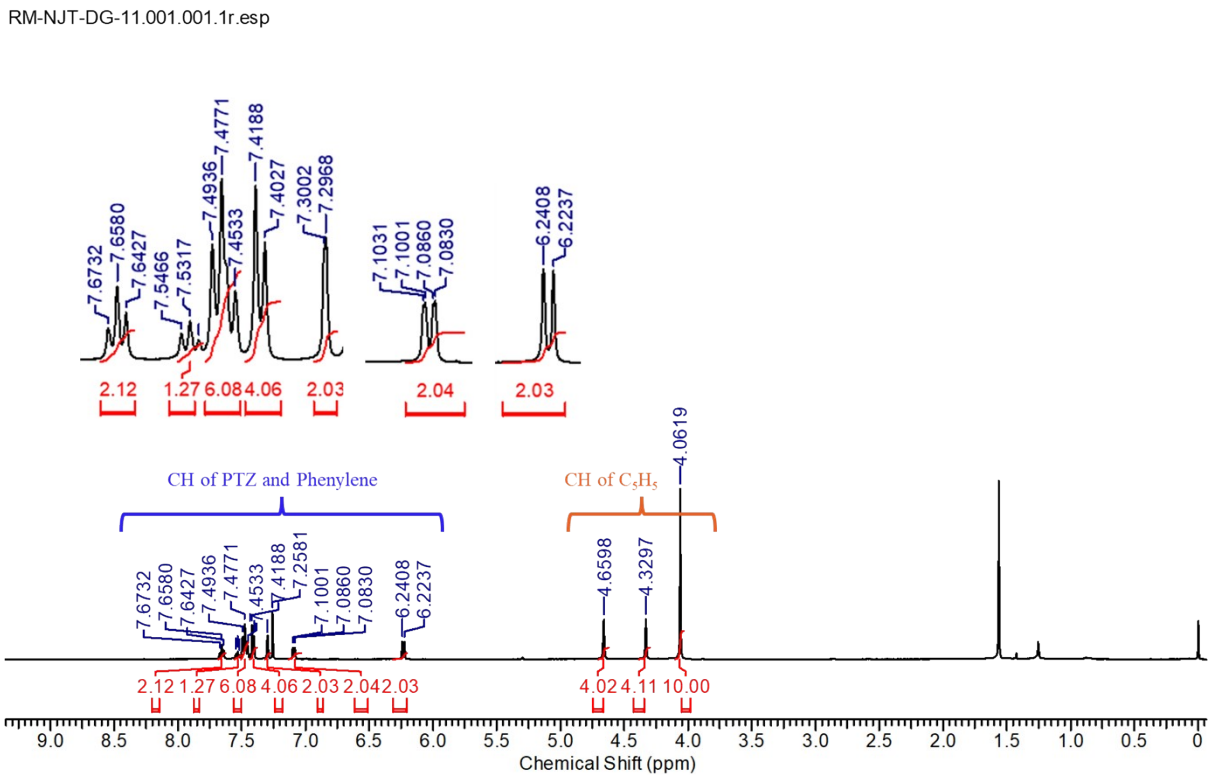

Fig. S19. ^{1}H NMR of **Fc2**.

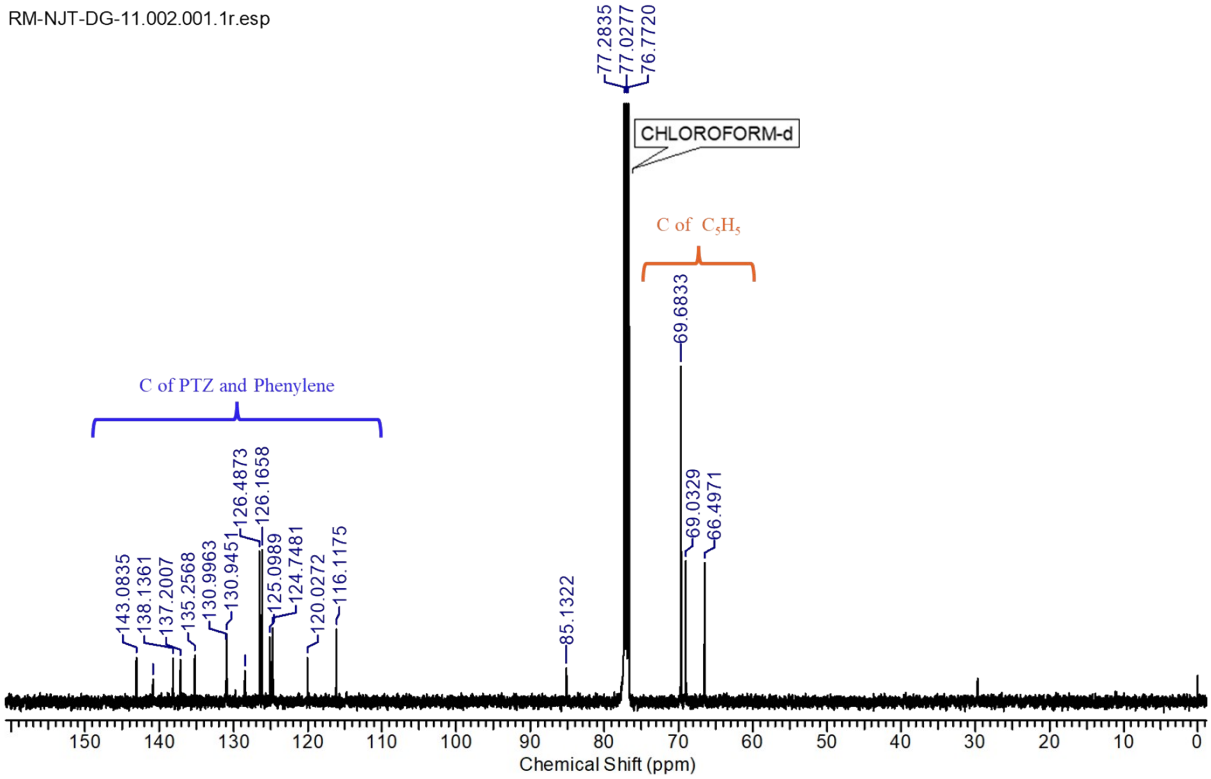

Fig. S20. ^{13}C NMR of **Fc2**.

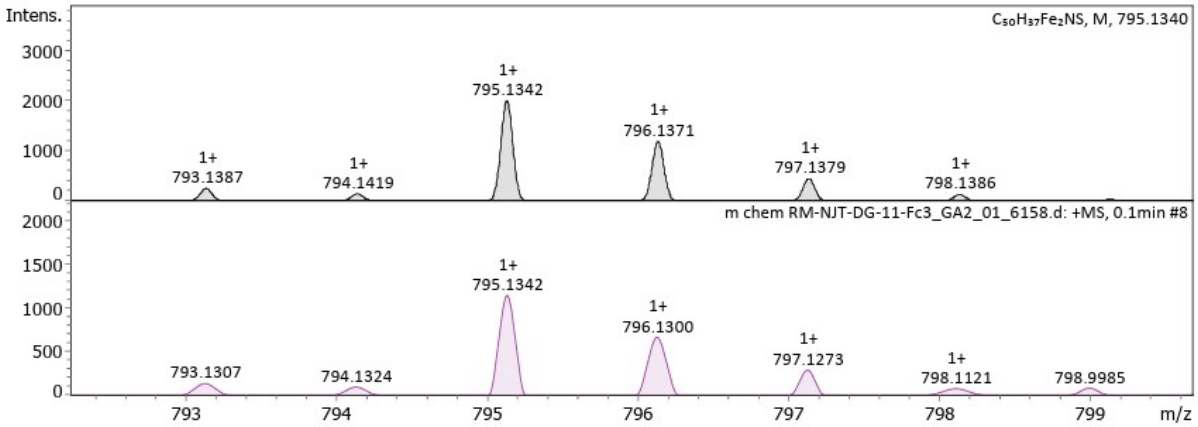

Fig. S21. HRMS of **Fc2**.

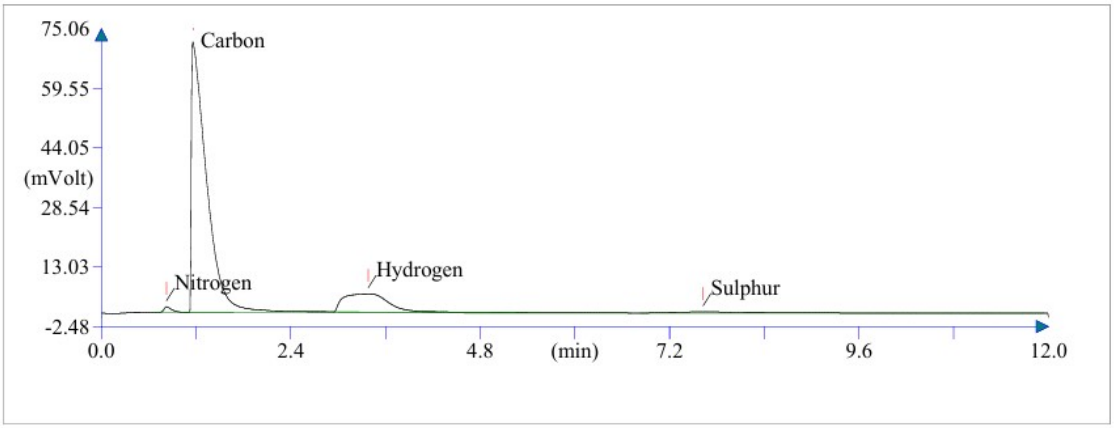

Operator ID:	
Company name:	ThermoFinnigan
Method filename:	C:\Eager for FLASH\04 JUL 24 CHNS\NCHS_19-12-2024.mth
Method name:	NCHS
Analysed:	22-01-25 12:35
Printed:	01-22-2025 15:06
Elemental Analyser method:	
Sampler method:	
Sample ID:	RM-DG-Fc-2 (# 32)
Analysis type:	UnkNown
Chromatogram filename:	22-01-25-03.dat
Calibration method:	K Factors
Sample weight:	2.439
Protein factor:	6.25

Component Name	Element %	Retention Time (min)	Area (.1*uV*sec)
Nitrogen	1.493	0.825	110374
Carbon	72.461	1.158	9762763
Hydrogen	4.630	3.383	1876367
Sulphur	3.314	7.625	177546
	81.898		11927050

Fig. S22. Elemental analysis of **Fc2**.

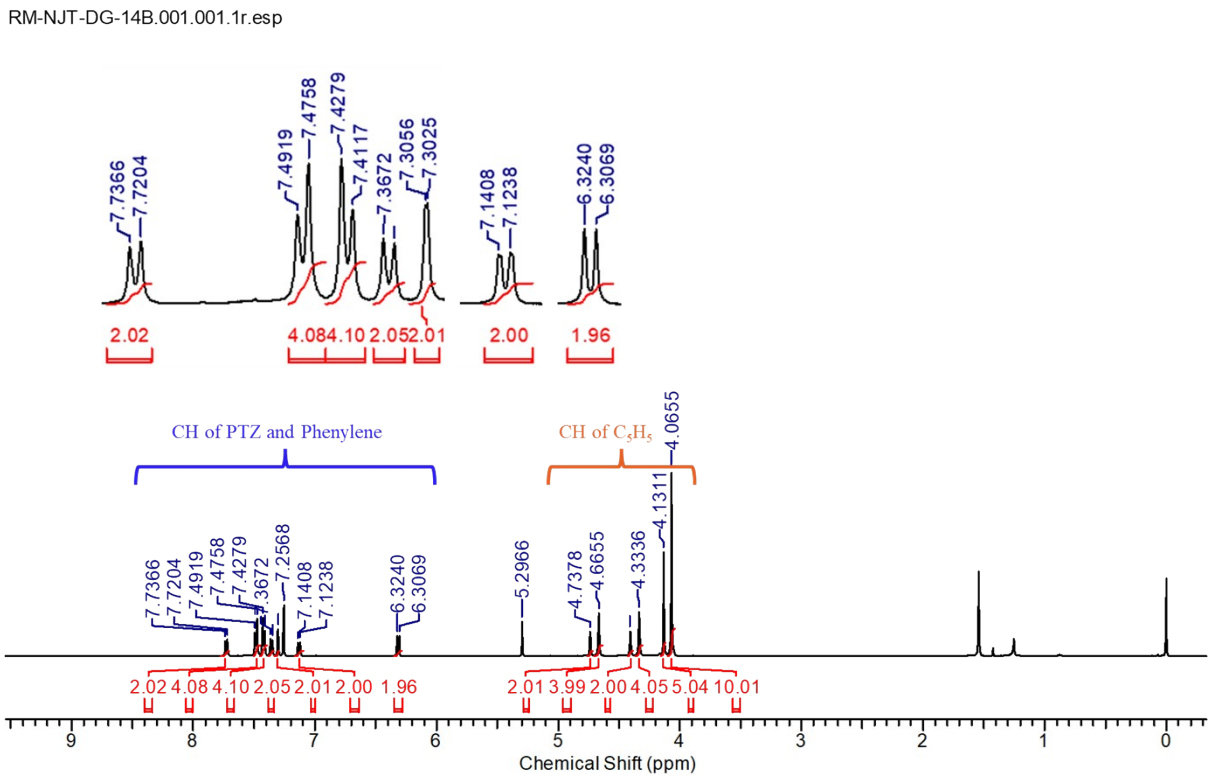

Fig. S23. ^{1}H NMR of **Fc3**.

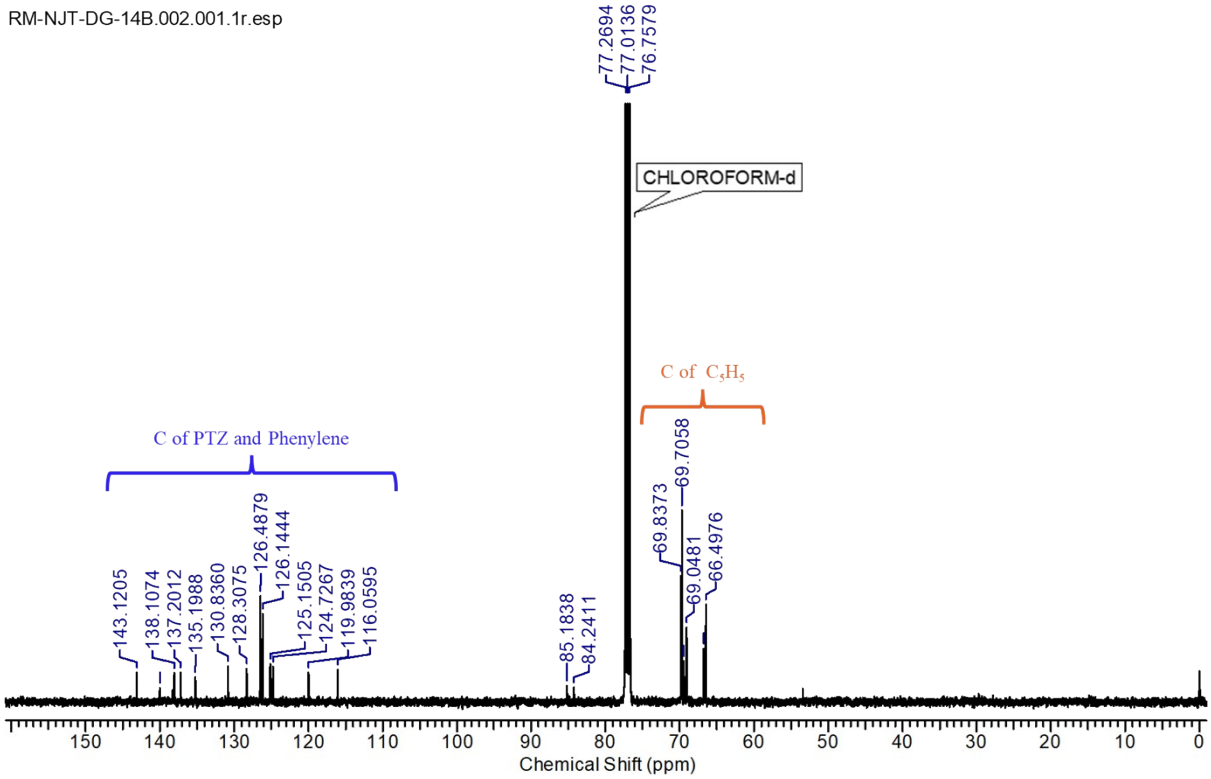

Fig. S24. ^{13}C NMR of **Fc3**.

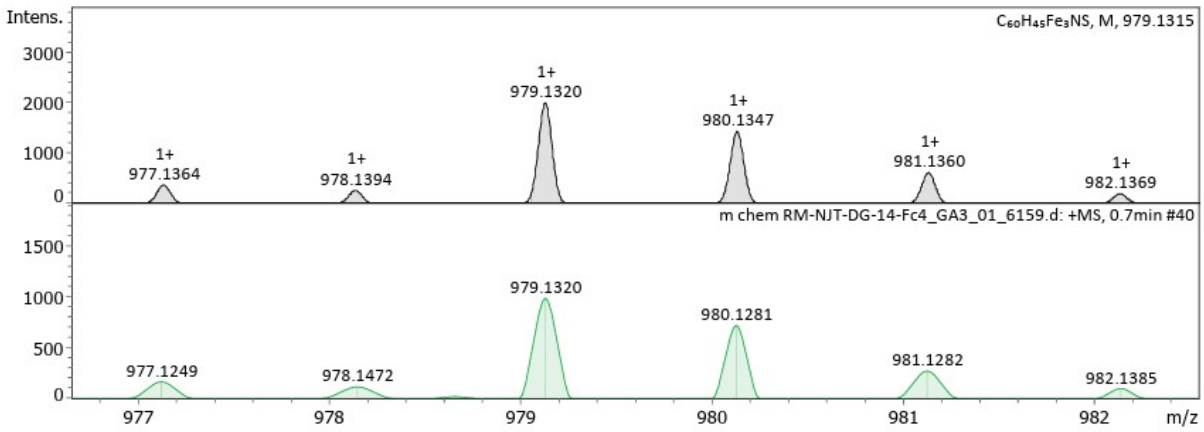

Fig. S25. HRMS of **Fc3**.

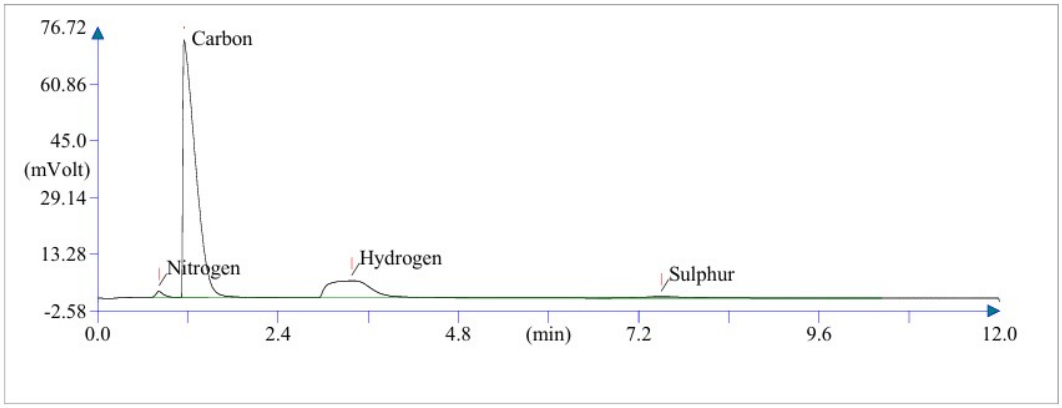

Operator ID:	
Company name:	ThermoFinnigan
Method filename:	C:\Eager for FLASH\04 JUL 24 CHNS\NCHS_19-12-2024.mth
Method name:	NCHS
Analysed:	22-01-25 12:48
Printed:	01-22-2025 15:07
Elemental Analyser method:	
Sampler method:	
Sample ID:	RM-DG-Fc-3 (# 33)
Analysis type:	UnkNown
Chromatogram filename:	22-01-25-04.dat
Calibration method:	K Factors
Sample weight:	2.235
Protein factor:	6.25

Component Name	Element %	Retention Time (min)	Area (.1*uV*sec)
Nitrogen	1.969	0.817	126610
Carbon	67.250	1.150	8303946
Hydrogen	5.371	3.383	1993926
Sulphur	3.271	7.500	160591
	77.860		10585070

Fig. S26. Elemental analysis of **Fc3**.

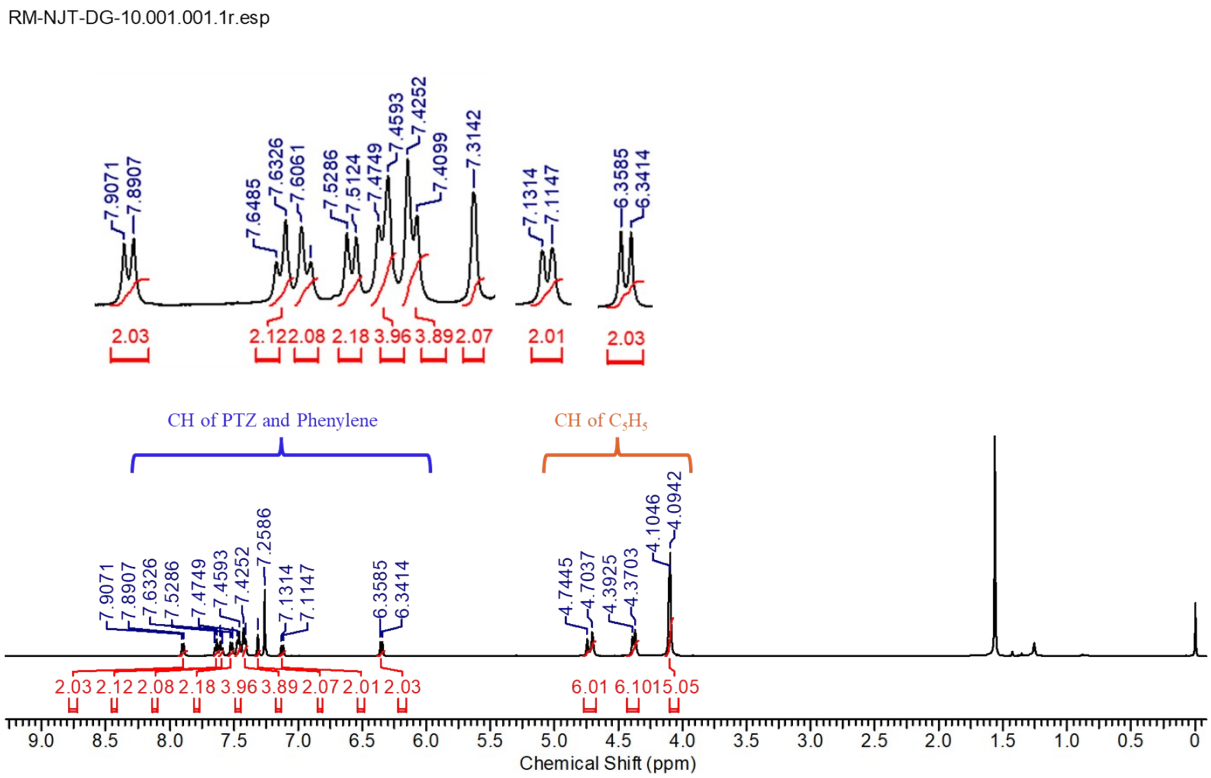

Fig. S27. ^{1}H NMR of **Fc4**.

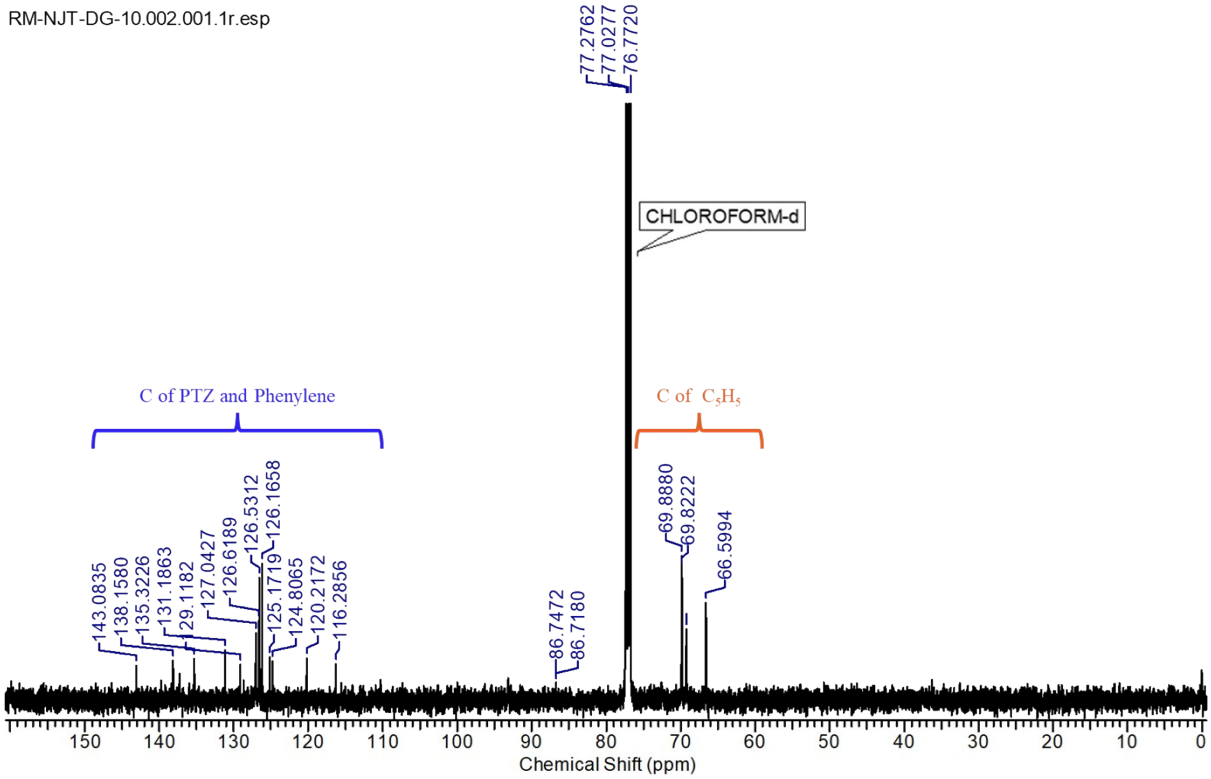

Fig. S28. ^{13}C NMR of **Fc4**.

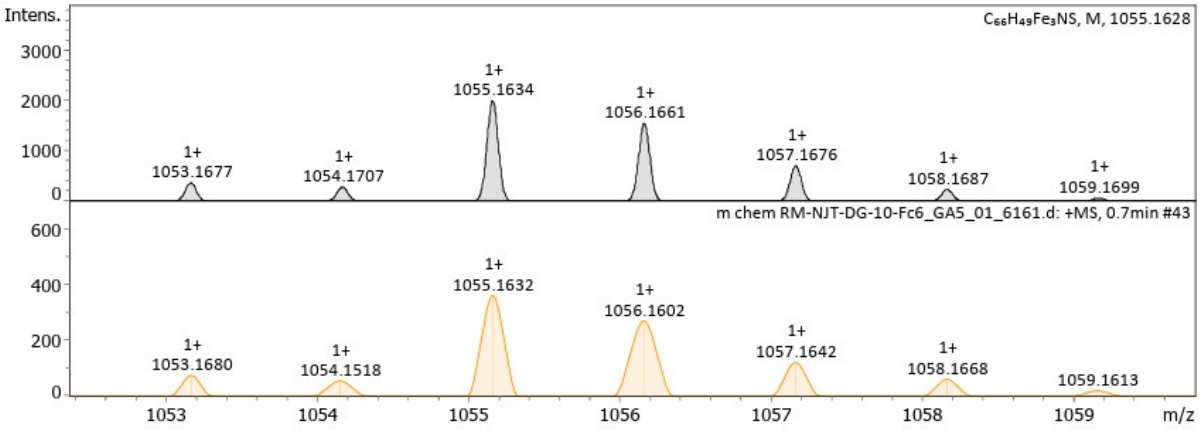

Fig. S29. HRMS of **Fc4**.

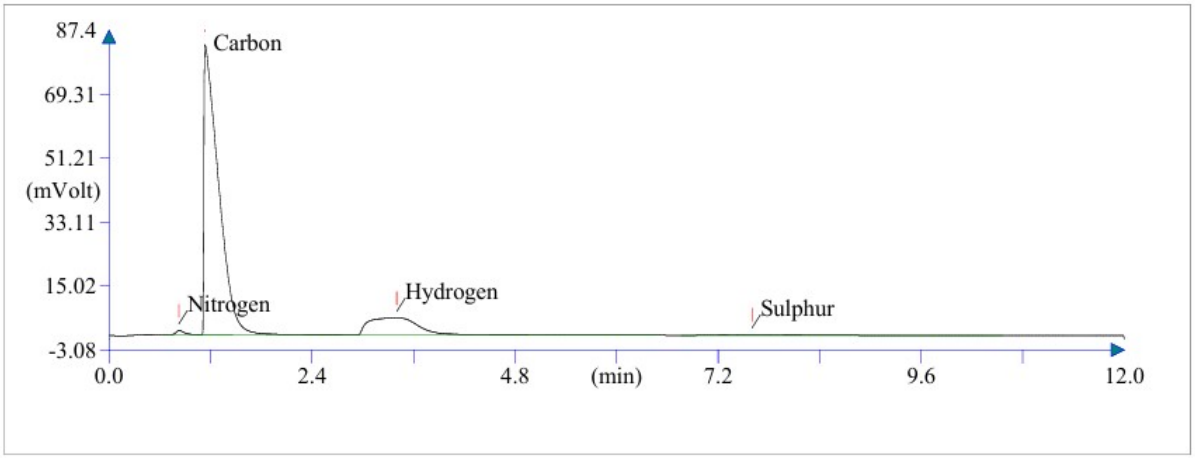

Operator ID:	
Company name:	ThermoFinnigan
Method filename:	C:\Eager for FLASH\04 JUL 24 CHNS\NCHS_19-12-2024.mth
Method name:	NCHS
Analysed:	22-01-25 13:00
Printed:	01-22-2025 15:07
Elemental Analyser method:	
Sampler method:	
Sample ID:	RM-DG-Fc-4 (# 34)
Analysis type:	UnkNown
Chromatogram filename:	22-01-25-05.dat
Calibration method:	K Factors
Sample weight:	2.433
Protein factor:	6.25

Component Name	Element %	Retention Time (min)	Area (.1*uV*sec)
Nitrogen	1.163	0.825	93062
Carbon	73.191	1.133	9836692
Hydrogen	5.064	3.400	2046307
Sulphur	2.607	7.600	139315
	82.025		12115380

Fig. S30. Elemental analysis of **Fc4**.

References:

1. Gaussian 09, Revision 09 W, M. J. Frisch, G. W. Trucks, H. B. Schlegel, G. E. Scuseria, M. A. Robb, J. R. Cheeseman, G. Scalmani, V. Barone, B. Mennucci, G. A. Petersson, H. Nakatsuji, M. Caricato, X. Li, H. P. Hratchian, A. F. Izmaylov, J. Bloino, G. Zheng, J. L. Sonnenberg, M. Hada, M. Ehara, K. Toyota, R. Fukuda, J. Hasegawa, M. Ishida, T. Nakajima, Y. Honda, O. Kitao, H. Nakai, T. Vreven, J. A. Montgomery, Jr., J. E. Peralta, F. Ogliaro, M. Bearpark, J. J. Heyd, E. Brothers, K. N. Kudin, V. N. Staroverov, R. Kobayashi, J. Normand, K. Raghavachari, A. Rendell, J. C. Burant, S. S. Iyengar, J. Tomasi, M. Cossi, N. Rega, J. M. Millam, M. Klene, J. E. Knox, J. B. Cross, V. Bakken, C. Adamo, J. Jaramillo, R. Gomperts, R. E. Stratmann, O. Yazyev, A. J. Austin, R. Cammi, C. Pomelli, J. W. Ochterski, R. L. Martin, K. Morokuma, V. G. Zakrzewski, G. A. Voth, P. Salvador, J. J. Dannenberg, S. Dapprich, A. D. Daniels, Farkas, J. B. Foresman, J. V. Ortiz, J. Cioslowski, D. J. Fox, Gaussian, Inc. Wallingford CT, 2009.
2. O. V. Dolomanov, L. J. Bourhis, R. J. Gildea, J. A. K. Howard, H. Pusch-mann, *J. Appl. Crystallogr.* 2009, **42**, 339–341.
3. G. M. Sheldrick, *Acta Crystallogr.* 2015, **71**, 3–8.
4. G. M. Sheldrick, *Acta Crystallogr.* 2008, **64**, 112–122.